

# Journal of Visualized Experiments

## Building An Enhanced Flight for the Study of Tethered Insect Flight

--Manuscript Draft--

<b>Article Type:</b>	Methods Article - JoVE Produced Video
<b>Manuscript Number:</b>	JoVE62171R1
<b>Full Title:</b>	Building An Enhanced Flight for the Study of Tethered Insect Flight
<b>Corresponding Author:</b>	Anastasia Bernat University of Chicago Division of Biological Sciences Chicago, IL UNITED STATES
<b>Corresponding Author's Institution:</b>	University of Chicago Division of Biological Sciences
<b>Corresponding Author E-Mail:</b>	anastabernat@gmail.com;avbernat@uchicago.edu
<b>Order of Authors:</b>	Anastasia Bernat
<b>Additional Information:</b>	
<b>Question</b>	<b>Response</b>
Please specify the section of the submitted manuscript.	Engineering
Please indicate whether this article will be Standard Access or Open Access.	Standard Access (US\$2,400)
Please indicate the <b>city, state/province, and country</b> where this article will be <b>filmed</b> . Please do not use abbreviations.	Chicago, IL, United States
Please confirm that you have read and agree to the terms and conditions of the author license agreement that applies below:	I agree to the <a href="#">Author License Agreement</a>
Please provide any comments to the journal here.	Thank you for all your comments.

**TITLE:**

Building an Enhanced Flight Mill for the Study of Tethered Insect Flight

**AUTHORS AND AFFILIATIONS:**

Anastasia Bernat

Department of Ecology and Evolution, University of Chicago, Division of the Biological Sciences,  
Chicago, IL, US

Corresponding Author:

Anastasia Bernat (avbernat@uchicago.edu)

**KEYWORDS:**

flight mill, makerspace, 3D printing, laser cutting, automation, flight assay

**SUMMARY:**

This protocol uses three-dimensional (3D) printers and laser cutters found in makerspaces in order to create a more flexible flight mill design. By using this technology, researchers can reduce costs, enhance design flexibility, and generate reproducible work when constructing their flight mills for tethered insect flight studies.

**ABSTRACT:**

Makerspaces have a high potential of enabling researchers to develop new techniques and to work with novel species in ecological research. This protocol demonstrates how to take advantage of the technology found in makerspaces in order to build a more versatile flight mill for a relatively low cost. Given that this study extracted its mill prototype from flight mills built in the last decade, this protocol focuses more on outlining divergences made from the simple, modern flight mill. Previous studies have already shown how advantageous flight mills are to measuring flight parameters such as speed, distance, or periodicity. Such mills have allowed researchers to associate these parameters with morphological, physiological, or genetic factors. In addition to these advantages, this study discusses the benefits of using the technology in makerspaces, like 3D printers and laser cutters, in order to build a more flexible, sturdy, and collapsible flight mill design. Most notably, the 3D printed components of this design allow the user to adjust the heights of the mill arm and infrared (IR) sensors to test insects of various sizes. The 3D prints also enable the user to easily disassemble the machine for quick storage or transportation to the field. Moreover, this study makes greater use of magnets and magnetic paint to attach insects to the machine with minimal stress. Lastly, this protocol details a versatile analysis of flight data through computer scripts that efficiently separate and analyze differentiable flight trials within a single recording. Although more labor-intensive, applying the tools available in makerspaces and on free, online 3D modeling programs can help researchers avoid costly, premade products with narrowly adjustable dimensions and can facilitate multidisciplinary and process-orientated practices. By taking advantage of the flexibility and reproducibility of technology in makerspaces, this protocol promotes creative flight mill design and inspires open science.

## INTRODUCTION:

Given how intractable the dispersal of insects is in the field, the flight mill has become a common laboratory tool to address an important ecological phenomenon – how insects move. As a consequence, since the pioneers of the flight mill<sup>1-4</sup> ushered in six decades of flight mill design and construction, there have been noticeable design shifts as technologies improved and became more integrated into scientific communities. Over time, automated data-collecting software replaced chart recorders, and flight mill arms transitioned from glass rods to carbon rods and steel tubing<sup>5</sup>. In the last decade alone, magnetic bearings replaced Teflon or glass bearings as optimally frictionless, and pairs between flight mill machinery and versatile technology have been proliferating as audio, visual, and layer fabrication technology become increasingly integrated into researchers' workflows. These pairings have included high-speed video cameras to measure wing aerodynamics<sup>6</sup>, digital-to-analog boards to mimic sensory cues for studying auditory flight responses<sup>7</sup>, and 3D printing to make a calibration rig to track wing deformation during flight<sup>8</sup>. With the recent rise of emerging technologies at makerspaces, particularly at institutions with digital media centers run by knowledgeable staff<sup>9</sup>, there are greater possibilities to enhance the flight mill to test a larger range of insects and to transport the device to the field. There is also a high potential for researchers to cross disciplinary boundaries and accelerate technical learning through production-based work<sup>9-12</sup>. The flight mill presented here (adapted from Attisano and colleagues<sup>13</sup>) takes advantage of emerging technologies found in makerspaces to not only 1) create flight mill components whose scales and dimensions are fine-tuned to the project at hand but also 2) offer researchers an accessible protocol in laser cutting and 3D printing without demanding a high-budget or any specialized knowledge in computer-aided design (CAD) models.

The benefits of coupling new technologies and methods with the flight mill are substantial, but flight mills are also valuable stand-alone machines. Flight mills measure insect flight performance and are used to determine how flight speed, distance, or periodicity relates to environmental or ecological factors, such as temperature, relative humidity, season, host plant, body mass, morphological traits, age, and reproductive activity. Distinct from alternative methods like actographs, treadmills, and the video recording of flight movement in wind tunnels and indoor arenas<sup>14</sup>, the flight mill is notable for its ability to collect various flight performance statistics under laboratory conditions. This helps ecologists address important questions on flight dispersal, and it helps them progress in their discipline – whether that be integrated pest management<sup>15-17</sup>, population dynamics, genetics, biogeography, life-history strategies<sup>18</sup>, or phenotypic plasticity<sup>19-22</sup>. On the other hand, devices like high-speed cameras and actographs can require a strict, complicated, and expensive setup, but they can also lead to more fine-tuned movement parameters, such as wing-beat frequencies and insect photophase activity<sup>23,24</sup>. Thus, the flight mill presented here serves as a flexible, affordable, and customizable option for researchers to investigate flight behavior.

Likewise, the incentive to integrate emerging technologies into ecologists' workflow continues to rise as questions and approaches to studying dispersal become more creative and complex. As locations that promote innovation, makerspaces draw in multiple levels of expertise and offer a low learning curve for users of any age to acquire new technical skills<sup>10,12</sup>. The iterative and collaborative nature of prototyping scientific devices in the makerspace and through online open

sources can accelerate the application of theory<sup>11</sup> and facilitate product development in the ecological sciences. Furthermore, increasing the reproducibility of scientific tools will encourage wider data collection and open science. This can help researchers standardize equipment or methods for measuring dispersal. It can allow researchers to unify dispersal data across populations in order to test metapopulation models that develop from dispersal kernels<sup>25</sup> or source-sink colonization dynamics<sup>26</sup>. Much like how the medical community is adopting 3D printing for patient care and anatomy education<sup>27</sup>, using laser cutters and 3D printers can redesign ecological tools and education and, within the scope of this study, can be used to design additional flight mill components, such as landing platforms or a flight mill arm that can move vertically. In turn, the customization, cost-effectiveness, and increased productivity offered by makerspace technology can help start up dispersal projects with a relatively low barrier for researchers who intend to develop their own tools and devices.

To construct this flight mill, there are also mechanical and instrumental limitations that can be considered by the maker. Magnets and 3D printed enhancements allow the flight mill to be essentially glueless, except for the construction of the cross brackets, and to be accommodable to insects of different sizes. However, as the mass and the strength of insects increase, insects may be more likely to dismount themselves while tethered. Strong magnets can be used at the cost of increased torsional drag, or ball bearings can replace magnetic bearings as a robust solution for flight testing insects that weigh several grams<sup>28,29</sup>. Nevertheless, ball bearings can also present some problems, mainly that running experiments with high speeds and high temperatures for long trial times can degrade the lubrication of ball bearings, which increases friction<sup>30</sup>. Thus, users will have to discern which flight mill mechanics would best suit their insect(s) of study and experimental design.

Similarly, there are several ways to instrument a flight mill that is beyond this paper's considerations. The flight mill presented in this paper uses IR sensors to detect revolutions, WinDAQ software to record revolutions, and programming scripts to process the raw data. Although it is easy-to-use, the WinDAQ software has a limited array of tools available - users cannot attach comments to their corresponding channel, and they cannot be alerted if any component of the circuitry fails. These cases are solved by detecting and correcting them through code but only after data collection. Alternatively, users can adopt more than one software that offers customizable data collection features<sup>28</sup> or sensors that take direct speed and distance statistics, like bike milometers<sup>29</sup>. However, these alternatives can bypass valuable raw data or diffuse functionality across too many software applications, which can make data processing inefficient. Ultimately, rather than refashioning flight mill instrumentation, this protocol offers robust programming solutions to present-day software limitations.

In this paper, a design for an enhanced simple flight mill is described to aid researchers in their dispersal studies and to encourage the incorporation of emerging technologies in the field of behavioral ecology. This flight mill fits within the constraints of an incubator, holds up to eight insects simultaneously, and automates data collection and processing. Notably, its 3D printed enhancements allow the user to adjust the mill arm and IR sensor heights to test insects of various sizes and to disassemble the device for quick storage or transportation. Thanks to



institutional access to a communal makerspace, all enhancements were free, and no additional costs were accrued compared to the simple, modern flight mill. All software needed are free, the electronic circuitry is simple, and all scripts can be modified to follow the specific needs of the experimental design. Moreover, coded diagnostics allow the user to check the integrity and precision of their recordings. Lastly, this protocol minimizes the stress sustained by an insect by magnetically painting and attaching insects to the mill arm. With the assembly of the simple flight mill being already accessible, affordable, and flexible, the use of makerspace technologies to enhance the simple flight mill can grant researchers the space to overcome their own specific flight study needs and can inspire creative flight mill designs beyond this paper's considerations.

## PROTOCOL:

### 1. Build the flight mill in a makerspace

#### 1.1 . Laser cut and assemble the acrylic plastic support structure.

1.1.1. Use 8 (304.8 mm x 609.6 mm x 3.175 mm) thick transparent acrylic sheets to construct the acrylic plastic support structure. Ensure that the material is not polycarbonate, which looks similar to acrylic but will melt instead of getting cut under the laser.

1.1.2. Locate the laser cutter in the makerspace. This protocol assumes the makerspace has a laser cutter, as referenced in the **Table of Materials**. For other laser cutters, read the laser cutter settings to determine what line color or thickness is needed to set the file lines to be laser cut or engraved (not to be rastered).

1.1.3. Open Adobe Illustrator, Inkscape (free), or another vector graphics editor. Prepare a file that reads the acrylic support design in a vector format with the aforementioned lines shown in **Figure 1**. Create file lines in Adobe Illustrator in Red, Green, and Blue (RGB) mode with a line stroke of 0.0001 point where RGB Red (255, 0, 0) cuts lines and RGB Blue (0, 0, 255) etches lines.

1.1.4. As a precaution, test and account for kerf for all slit and hole measurements. Design and test the kerf key (**Supplemental Figure 1**).

NOTE: The measurements can vary based on the beam width of the laser cutter, the width of the material, and the material type used.

1.1.5. To allow the software to read, save the acrylic support designs and kerf key as file types such as .ai, .dxf, or .svg files. To send the job to the laser cutter, print the file on the laser cutter's local machine and then open the laser software.

NOTE: If printed correctly, all the vector cutting lines in the design will appear with the appropriate corresponding colors in the laser software's control panel.

1.1.6. Select the material as **Plastic** and then the material type as **Acrylic**. For extra precision, measure the material thickness with a caliper and enter its thickness into the material thickness field. Auto-enable the Z-axis of the material's focal point. Set the **Figure Type** to **None** and leave the **Intensity** at **0%**. To change any advanced metrics on the laser cutter, such as the laser % Power or % Speed, test with the kerf key.

NOTE: The rule of thumb is that the thicker the material, then the more power is required at a lower speed.

1.1.7. Before cutting, follow the makerspace's guidelines on powering up, using, and maintaining the laser cutter. Place the materials in the printer cavity and cut the acrylic supports.

NOTE: To prevent possible eye damage, do not look at the laser or leave any acrylic sheet unattended while cutting.

1.1.8. Clean excess material out of the printer cavity and assemble the support structure. Assemble by inserting each horizontal shelf into the open slits of the outside vertical walls and central vertical wall as labeled in **Figure 2A**. Ensure that the holes between the horizontal shelves are aligned.

## 1.2. 3D print the plastic supports

1.2.1. Open a web browser and create a free account on an online 3D modeling program.

1.2.2. Click on **3D Designs > Create** a new design. To replicate this study's exact 3D printed designs as seen in **Figure 3**, download the archive **3D\_Prints.zip (Supplemental 3D Prints)**, and move the folder onto the desktop. Unzip and open the folder. In the online 3D modeling program workplane webpage, click on **Import** in the top right corner and select the **.stl file(s)**.

NOTE: Multiple design replicates or objects can fill the workplane and be saved as a single .stl file as long as the user restrains the objects within the boundaries of the build area of the 3D printer. The largest object a 3D printer can print is 140 mm length x 140 mm width x 140 mm depth. However, do not rotate the objects along their z-axis as a means to maximize the number of objects on a build area. That is because the downloaded objects have been positioned to minimize overhangs, and so they can be printed optimally with the minimal necessary supports.

1.2.3. To self-create or make adjustments to the designs, follow the website's tutorials, make edits, and then export the new designs as .stl files. In total, 8 linear guide rails (100.05 mm length x 23.50 mm width x 7.00 mm depth), 16 linear guide rail blocks (22.08 mm length x 11.47 mm width x 12.47 mm depth), 12 to 20 screws (9.00 mm length x 7.60 mm width x 13.00 mm depth), 15 cross brackets (50.00 mm length x 50.00 mm width x 20.00 mm depth), 16 magnet holders (12.75 mm length x 12.50 mm width x 15.75 mm depth), 16 tube supports (29.22 mm length x 29.19 mm width x 11.00 mm depth), 16 short linear guide rail supports (40.00 mm length x 11.00 mm width x 13.00 mm depth), and 16 long linear guide rail supports (40.00 mm length x 16.00

mm width x 13.00 mm depth) need to be 3D printed. To obtain the mirror of each linear guide rail design, click on the object, press **M**, and select the arrow corresponding to the object's width.

NOTE: See step 1.3.6. for more information on the linear guide rail pegs.

1.2.4. Download and install a 3D printing slicing software to convert .stl files to a 3D printer readable .gx file. Refer the **Table of Materials** to download the free software program.

NOTE: Other conversion software programs are acceptable, but this protocol assumes the makerspace is using the 3D printer and printing slicing software as referenced in the **Table of Materials**.

1.2.5. Double-click the icon of the 3D printing slicing software to start the software. Click **Print > Machine Type** and select the **3D printer** that is located in the makerspace.

1.2.6. Click the **Load** icon to load a .stl model file and display the object on the build area.

1.2.7. Select the object and double-click the **Move** icon. Click **On Platform** to ensure that the model is on the platform. Click **Center** to place the object at the center of the build area or drag the object with the mouse pointer to position the object on the build area.

1.2.8. Click on the **Print** icon. Ensure that **Material Type** is set to **PLA**, supports and raft are enabled, **Resolution** is set to **Standard**, and the temperature of the extruder matches the temperature suggested by the 3D printer guide. The temperature can be changed within **More Options >> Temperature**.

1.2.9. Press **OK** and save the .gx file in the **3D\_Prints folder** or on a USB stick if the file cannot be transferred to the 3D printer through a USB cable.

1.2.10. Locate a makerspace's 3D printing machine. Calibrate the extruder and ensure that there is enough filament for printing. Transfer the .gx file to the 3D printer and print all types and quantities of plastic supports and enhancements. For each print, check that the filament is sticking properly to the plate.

1.3. Assemble 3D prints onto the acrylic support structure.

1.3.1. To visualize all the supports in place, see **Figure 2B**.

1.3.2. Hot glue the 3.175 mm thick neoprene sheets onto the interior walls of the cross bracket. When dry, insert the cross brackets at the junctions of the acrylic shelves and the walls at the back of the device to stabilize the flight mill.

1.3.3. Wherever possible, use 3D printed screws in order to minimize the magnetic influence of iron screws. Screw in the tube supports onto the bottom and the top of each cell. Ensure that the top and bottom tube supports are aligned.

1.3.4. Insert a 30 mm long plastic tube (inner diameter (ID) 9.525 mm; outer diameter (OD) 12.7 mm) into the top tube support and a 15 mm long plastic tube (ID 9.525 mm; OD 12.7 mm) into the bottom tube support of each cell. Then, insert a 40 mm long plastic tube (ID 6.35 mm; OD 9.525 mm) into the top tube and a 20 mm long plastic tube (ID 6.35 mm; OD 9.525 mm) into the bottom tube. Ensure that there is strong enough friction between the tubes to hold the tubes in place, but not too much that the inner tube can still slide up and down if pulled on. If tubes are warped, submerge segments of the tubes for 1 min in boiling water. Straighten the tubes out on a towel, allow it to reach room temperature and then insert the tubes.

1.3.5. Place the two low-friction neodymium magnets (10 mm diameter; 4 mm length; 2.22 kg holding force) and an inner tube into each magnet support. Check if each pair of magnets is repelling each other. Additionally, lodge the inner tube firmly lodged into each magnet support so that gravity acting on the magnets and the magnet support is not strong enough to dislodge them from the inner tube.

1.3.6. Facing the same direction, slide two linear guide rail blocks into the linear guide rail. Lodge the linear guide rails and blocks upright into the windows on the outer vertical walls. Ensure that the block openings are facing upwards. To secure one linear guide rail in place, use two short linear guide rail supports, two long linear guide rail supports, four 10 mm long iron screws (M5; 0.8 thread pitch; 5 mm diameter), two 20 mm long iron screws (M5; 0.8 thread pitch; 5 mm diameter), and two hex nuts (M5; 0.8 thread pitch; 5 mm diameter). **Figure 2C** shows the full assembly of linear guide rail.

NOTE: Open slots in the linear guide rail are intended to be used if and only if the linear guide rail becomes eroded by the repeated sliding of its block. If so, 3D print a small T-shaped peg found in the 3D\_Prints folder.

1.4. Construct the pivoting arm.

NOTE: Sub-sections 1.4.1 and 1.4.2 are equivalent to sub-sections 1.2.2. and 1.2.3. in Attisano et al. 2015 methods paper<sup>13</sup>.

1.4.1. Puncture the filter of a 20  $\mu$ L filtered pipette tip at its center point using an entomological pin. Then, push the pin through the pipette tip until the steel ends of the pin protrude from the body of the pipette tip. Ensure that the filter of the pipette tip secures the pin in place. The pin serves as the axis of the flight mill arm.

1.4.2. To maximize cell space, cut a 19 G non-magnetic hypodermic steel to a length of 24 cm (1 cm less than the width of a flight cell). Hot glue the protruding pin and the crown of the pipette

tip from step 1.4.1. to the midpoint of the tubing. Bend one end of the tubing at 2 cm from the end to an angle of 95°.

NOTE: To prioritize insect size rather than maximize cell space, shorten the radius of the arm for smaller insects or weak flyers. A longer flight arm can also be assembled if the center acrylic wall is removed for larger insects or strong flyers. Moreover, the bent ending of the arm can support different angles in order to position the insect in its natural flight orientation.

1.4.3. To test its magnetic suspension, position the arm between the top set of magnets. Ensure that the rotating arm spins freely around the vertically suspended pin.

1.4.4. Glue the two low-friction neodymium magnets (3.05 mm diameter; 1.58 mm length; 0.23 kg holding force) on the bent end of the pivot arm to tether the metal-painted insect for flight (mass of flight mill arm with magnets = 1.4 g). On the unbent end of the pivot arm, wrap a piece of aluminum foil (mass per area = 0.01 g/cm<sup>2</sup>) to create a flag. The foil flag acts as a counterweight, and, due to its highly reflective properties, it optimally breaks the IR beam sent from the IR sensor transmitter to the receiver.

NOTE: The diameter of the IR beam is at most 2.4 mm, so the optimal minimum width of the foil flag is 3 mm. A foil flag width of 3 mm and positioned to break the beam of IR light in front of the sensor's emitter lens will produce a drop in voltage that is detectable during analyses.

1.5. Set up the IR sensor and data logger.

1.5.1. Place the IR sensor transmitter inside the top linear guide rail block with the emitter of the beam facing downwards. Then, place the IR sensor receiver inside the bottom block facing upwards.

NOTE: The sensors (20 mm length x 10 mm width x 8 mm depth) can be separated up to a distance of 250 mm and still function; therefore, they will function even when positioned at the ends of the approximately 100 mm linear guide rail.

1.5.2. On a solderless breadboard, connect the IR sensor transmitter and receiver in series with the 4-channel analog input data logger, as shown in the electronic circuit in **Figure 4A**. Connect the IR sensor transmitter (not the receiver) input first, following the 180 Ω resistor. Place another 2.2 kΩ resistor before the output of the IR receiver connection. Configure each channel's electronic circuit in alternate rows along the breadboard to minimize noise in the voltage signal from multiple sensors during recording (**Figure 4B**).

## 2. Conduct Flight Trials

2.1. Magnetically tether insects to the flight mill arm.

2.1.1. To minimize stress placed on the insect, apply magnetic paint on the insect's pronotum using either a toothpick or a fineline precision applicator (20 G tip). Let the paint dry for at least 10 min. Once dry, attach the insect to the flight mill arm magnets. Refer **Figure 5** to see examples of magnetic application and tethering for insects of different sizes. This protocol uses *Jadera haematoloma* (soapberry bug) as the model insect for flight tethering and trial experimentation.

NOTE: For a stronger attraction between the insect and the arm magnets, apply multiple layers of magnetic paint. Additionally, swap out the magnets attached to the end of the flight mill arm for magnet sizes that best accommodate the insects' field of vision, mass, and wing range.

2.1.2. Flow up to 8 insects at a time in the flight mill. Paint prep at least 16 insects in order to test multiple insects sequentially during a single recording session.

2.1.3. To remove the magnetic paint after testing, chip off the paint with fine forceps and dispose of it according to Environmental Protection Agency (EPA) and Occupational Safety and Health Administration (OSHA) regulations.

2.2. Record multiple insects sequentially without terminating a recording session using WinDAQ's Event Marker Comment tool.

2.2.1. Download and install the free WinDAQ Data Recording and Playback Software.

2.2.2. Create a new folder titled **Flight\_scripts** on the desktop. Create five new folders with the following exact names inside the **Flight\_scripts** folder: **data**, **files2split**, **recordings**, **split\_files**, and **standardized\_files**. Download the **datasheet.xlsx** (**Supplemental File 1**) and drag the file into the data folder in the **Flight\_scripts** directory.

2.2.3. Use the **datasheet.xlsx** as a manual data-recording template. A minimum of four columns is needed: the identification number of the bug, whether the bug died before being tested, the recording set number, and the chamber comprised of the channel letter and channel number (e.g., 'A-1', 'B-4'). Refer **Figure 2A** for one possible chamber configuration.

2.2.4. Open the **WinDAQ Dashboard**, select the data-logger(s) from the checkbox list, and press '**Start Windaq Software**'. A new window will open for each data-logger selected, and the input signal from each sensor will be shown.

2.2.5. To start a new recording session, press **File > Record**. Select the location of the recording file in the first pop-up window. Write the file name carefully. Files have to have at least the following in their names: the recording set number and channel letter. An example of a filename modeled in the Python scripts is the following: **T1\_set006-2-24-2020-B.txt**. Refer to **split\_files.py** lines 78-87 from the **Flight\_scripts** folder to get further details. Then, press **OK**.

2.2.6. In the next pop-up window, enter the anticipated length of the flight recording. Press **OK** when the insects are in a position to begin flight. After the recording time, press **Ctrl-S** to finalize the file. Do not press **Ctrl-S** unless there is a need to terminate the recording early.

NOTE: If the file terminates too early either by typing **Ctrl+S** or the aforementioned length of time was too short, append a new recording to an existing file by clicking on **File > Record**. Select the file to append to and click **Yes** on the following pop-up window.

2.2.7. When pulling out tested insects during the recording, insert a commented event marker of the incoming insect at its selected chamber. Always manually record the ID, chamber, and recording set of the incoming insect in **datasheet.xlsx** before swapping insects.

2.2.8. To make an event marker comment, click on the channel number. Then, click **Edit > Insert Commented Mark**. Define the comment with the identification number of the new insect entering the chamber. Press **OK** and load the insect into the chamber.

### 2.3. Visualize event marker comments and convert file from WDH to TXT.

2.3.1. Visualize event marker comments by going to **Edit > Compression...** and then click the **Maximum** button to fully compress the waveform into one window (**Figure 6A**).

2.3.2. Check for any abnormalities in the recording.

NOTE: The types of abnormalities or failures in the recording are displayed in **Figure 6**. These are diagnosed later and corrected in the Python scripts.

2.3.3. Save the file in a .txt format by going to **File > Save As**. Select the recordings folder inside the **Flight\_scripts** directory as the location to save the file. Select the file type as **Spreadsheet print (CSV)** in the pop-up window and write the filename with .txt at the end. Click **Save**. In the following pop-up window, select **Sample Rate**, **Relative Time**, and **Date and Time**. Type **1** in between **Channel Number** and **Event Markers**. Deselect all other options and click **OK** to save the file.

## 3. Analyze Flight Data

3.1. Split files by event marker comments.

3.1.1. Install the latest version of Python. All scripts in this protocol were developed on Python version 3.8.0.

3.1.2. Download the following Python scripts: **split\_files.py**, **standardize\_troughs.py**, and **flight\_analysis.py** (**Supplemental Coding Files**). Move the scripts into the **Flight\_scripts** folder.

3.1.3. Ensure that Python is up to date and install the following libraries: csv, os, sys, re, datetime, time, numpy, math, and matplotlib.pyplot. To observe the main functions and data structures of the scripts, see the schematic in **Supplemental Figure 2**.

3.1.4. Open the **datasheet.xlsx** file and save as a **CSV** by changing the file format to **CSV UTF-8 (Comma delimited)** if running Windows or **Macintosh Comma Separated** if running Mac.

3.1.5. Open the **split\_files.py** icon with the text editor of choice. If there is no preference, right-click on the script icon and select **Open with IDLE**.

3.1.6. Recode lines 133-135 and 232-233 if the user wrote a filename different from the suggested template ('T1\_set006-2-24-2020-B.txt'). To record the script to accommodate different filenames using the split() function see lines 116-131.

3.1.7. In line 266, type the path to the Flight\_scripts folder, and run the script. After a successful run, the script generates intermediate .txt files of mapped insect IDs in the files2split folder and .txt files for each insect tested in each recording set in the split\_files folder, within the Flight\_scripts directory.

NOTE: Additionally, in the Python Shell, users should see print statements of the filename, which insects are being swapped at a numbered event marker, and which files are being split and generated into new files by insect ID.

3.2. Standardize and select the troughs in the recorded signal

3.2.1. Open the **standardize\_troughs.py** icon with the text editor of choice. If there is no preference, right-click on the script icon and select **Open with IDLE**.

3.2.2. In line 158, type the sampling frequency (Sample/second).

NOTE: This protocol suggests 100 S/s because troughs, which are drops in voltage resulting from the flag interrupting the IR sensor beam, will still reach a minimum drop in voltage of 0.36 V for speeds of 1.7 m/s. In turn, noise, which has a maximum drop in voltage of 0.10 V, can still be filtered during standardizations without filtering real troughs. Additionally, a sample rate of 100 S/s makes it easy for the user to see the troughs on the on-screen waveform during and after recording. If errors happen during the recording, then the user can quickly discern the troughs from errors or noise. See **Supplemental Figure 3** for comparisons among several low sampling frequencies.

3.2.3. In line 159, type the path to the Flight\_scripts folder, and run the script. If the script successfully runs, it generates files in the standardized\_files folder in the Flight\_scripts directory.

NOTE: All files should start with the 'standardized\_' and end with the original filename.



3.2.4. **Check the quality of the recordings:** Open the **trough\_diagnostic.png** generated by the **standardize\_troughs.py** located in the **Flight\_scripts** folder. Ensure that all records are robust to changes in the minimum and maximum voltage value of the mean standardization interval.

NOTE: Recordings may have a lot of noise or have overly sensitive troughs if they exhibit large decreases in the number of troughs identified and counted when the minimum and maximum deviation values are increased. Additional diagnostics for the min-max normalization factor can also be coded, performed, and plotted. An alternative method for checking recording quality is described in steps 2.3.1. and 2.3.2. of the Attisano et al. 2015 methods paper<sup>13</sup>.

3.2.5. Assess the diagnostics, uncomment out line 198 and specify the minimum and maximum deviation values, which define the minimum and maximum values around the mean voltage used to perform the standardization for all files. The default is deviation values of 0.1 V.

NOTE: In line 53, the user can also specify the min-max normalization factor threshold in order to identify a voltage far below the threshold value.

3.2.6. Comment out line 189 after inputting the deviation values, and then run the script. The script will run the standardizations efficiently for all files (nearly 25 times faster).

3.3. Analyze the flight track using the standardized file.

3.3.1. Open the **flight\_analysis.py** icon with the text editor of choice. If there is no preference, right-click on the script icon and select **Open with IDLE**.

3.3.2. In lines 76-78, edit the optional speed correction that suppresses additional rotations of the mill's arm after an insect stops flying. Determine this threshold value with caution when working with slow flying insects.

3.3.3. In line 121, edit the speed thresholds to correct for false speed readings such as extremely fast speeds or negative speeds. In line 130, edit the time gap value to filter out long gaps that occur between two consecutive uninterrupted flying bouts.

3.3.4. In line 350, type the path to the folder in which the \*.txt standardized files are saved.

3.3.5. In line 353, input the arm radius length used during trials, which defines the circular flight path flown per revolution by the insect.

3.3.6. Identify the distance and time SI units as a string in lines 357 and 358.

3.3.7. In lines 388-397, use the **split()** function to extract, at a minimum, the insect's identification number and the set number and chamber in which the insect flew from the filename. The script follows the comprehensive filename example of 'standardized\_T1\_set006-

2-24-2020-B.txt'. If necessary, simplify this filename as suggested in step 2.2.5., and comment out or delete variables like trial type on lines 392 and 401, if not used.

3.3.8. Specify all the user settings, save and run the script. If the script run is successful, it prints the insect's corresponding ID number, chamber, and calculated flight statistics in the Python Shell. Additionally, it generates a comprised flight\_stats\_summary.csv file of the information printed in the Python Shell in the data folder of the Flight\_scripts directory.

#### REPRESENTATIVE RESULTS:

Flight data were obtained experimentally during Winter 2020 using field collected *J. haematoloma* from Florida as the model insects (Bernat, A. V. and Cenzer, M. L. , 2020, unpublished data). Representative flight trials were conducted in the Department of Ecology and Evolution at the University of Chicago, as shown below in **Figures 6–9**. The flight mill was set up within an incubator set to 28 °C/27 °C (day/night), 70% relative humidity, and a 14 h light/10 h dark cycle. For each trial, the flight track of multiple bugs was recorded every hundredth of a second by the WinDAQ software for up to 24 h. After preliminary trials, flight behavior was categorized into bursting flight and continuous flight. Bursters flew sporadically for less than 10 min at a time, and continuous flyers flew uninterrupted for 10 min or longer. Any individual that did not exhibit continuous flight behavior within its 30 min testing phase was pulled off the flight mill and replaced with a new bug and its accompanying ID in an event marker comment. All bugs that exhibited continuous flight remained on the flight mill beyond 30 min until they stopped flying. Bugs were swapped from 8 AM to 4 PM each day. As represented in **Figure 9**, flight trials of individuals in a day's recording varied in length from 30 min to 20+ h. By inserting event markers at the addition of new individuals, this complex data structure becomes successfully processed through the Python scripts, and the code effectively helps users visualize the scope of their experiments. The proposed experimental setup captures the full flight capacity of insects; however, it omits the possibility of observing flight periodicity. Users then have the option to tailor their flight trials for different flight metrics and choose which flight behavior or strategies they most wish to test.

The on-screen waveform and diagnostic heatmap(s) also make it possible to identify gaps or resolve inconsistencies in the flight track data. **Figure 6A** shows a set of trials whose flight data were successfully recorded for all channels without noise or disruption. It also shows all the event marker comments made during recording. **Figure 6B** shows a moment where the recorded signal was lost in channel 3, dropping the voltage immediately to 0 V. This was possibly due to the crossing over of open wires or the loosening of wires. There are also particular events during recording that could occur but are corrected for in the Python scripts. This includes double troughs, mirror troughs, and voltage noise (**Figure 6C,D**). These events lead to false trough readings, but they can reliably be identified and removed during analyses. **Figure 7** compares three data files to show how noise or sensitive troughs in the recording data were diagnosed during the standardization process. The first (**Figure 7A**) is a file whose troughs generated by each revolution of the flight mill arm were robust, meaning they largely deviated from the file's mean voltage. In turn, as the standardization interval around the mean increased, there was no change in the number of troughs identified. This suggested that there was no voltage noise, and the user

can then be confident in the accuracy of the standardization. On the other hand, the third file (**Figure 7C**) had troughs that were either too sensitive or had extraneous voltage noise that did not deviate largely from the file's mean voltage. As a result, its number of troughs decreased substantially as the standardization interval around the mean increased. It would then be advisable to look back into the original WDH recording file to confirm whether the insect was truly flying.

By plotting the flight speed and duration statistics of the individual, flight behavior can be further characterized into four flight categories: bursts (B), bursts to continuous (BC), continuous to bursts (CB), and continuous (C), as represented in **Figure 8**. An individual that strictly exhibited continuous flight flew uninterrupted for 10 min or more at least by the end of its 30 min testing phase (**Figure 8A**). An individual that flew sporadically throughout its 30 min testing phase exhibited bursting flight (**Figure 8B**). An individual that initially exhibited continuous flight for more than 10 min and then tapered within its 30 min testing phase into sporadic bursts exhibited continuous to bursting flight (**Figure 8C**). Finally, an individual that initially demonstrated bursting flight and then transitioned into continuous flight for the remainder of the 30 min testing phase and beyond exhibited bursting to continuous flight (**Figure 8D**). Thus, specific to the model insect and experimental framework, the user can use this graphic output to assess and identify general flight behavior patterns despite unique variations in individual tracks.

#### FIGURE AND TABLE LEGENDS:

**Figure 1: Designs to be laser cut for acrylic plastic sheet structure.** Eight acrylic plastic sheets were laser cut in order to construct the plastic support structure of the flight mill. File lines were created in Adobe Illustrator in RGB mode, where RGB Red (255, 0, 0) cut lines and RGB Blue (0, 0, 255) etched lines. For greater legibility in this figure, file line strokes were increased from 0.0001 point to 1 point. Coordinate units are mm, and the dot in the top left corner of each design is the origin, where moving further down and to the right of the origin leads to positive ascending values. There are three different sheet designs: the outside vertical walls, a central vertical wall, and horizontal shelves. The two outside vertical walls slide into the horizontal shelves at their slits, and their rectangular holes are used to mount the 3-D printed linear guide rail, blocks, and supports. There is one central vertical wall with slits that divides the flight mill into eight cells and provides additional structural support. There are also five horizontal shelves with slits, etched circles to mark the location of the magnetic tube supports, and small rectangular holes to allow the tube supports to be screwed in.

**Figure 2: Assembled flight mill. A)** Flight mill assembly. Each horizontal shelf (HS) has been inserted into the open slits of the outside vertical walls (OW) and central vertical wall (CW). Moreover, each cell, or 'chamber', is identified with a channel letter (A or B) that corresponds to a data logger and a channel number (1-4) that corresponds to the channel on the specific data logger. **B)** Flight mill cell assembly with flight mill arm. Magnetic bearings can be raised or lowered by sliding the inner tubes within the outer tubes to adjust the height of the arm. The IR sensors can be also be raised or lowered to align the sensors with the height of the flag on the arm. IR sensors can also be removed from their linear guide rail blocks easily if they need to be replaced

or inspected or if the flight mill needs to be transported. Cross brackets provide structural support for each acrylic cell and can be easily inserted and removed. **C)** Linear guide rail and block assembly in the cell window. All 3D components and respective screws in the cell window are labeled for clearer assembling.

**Figure 3: 3D printed designs.** Measurements are in mm. **A)** Linear guide rail. **B)** Linear guide rail block shaped to hold an IR sensor. **C)** Screw used as support to replace iron screws. **D)** Tube support. **E)** Magnet support. **F)** Cross bracket used as an acrylic frame aligner and stabilizer. **G)** Long support and **H)** short support to keep the linear guide rails in place. Only linear guide rail supports that rest on the outside face of the acrylic wall are shown. Linear guide rail support mirrors are not shown.

**Figure 4: Flight mill electrical circuitry.** **A)** Simple diagram of an electric circuit connecting the IR sensors to the data logger. When the flag on the mill arm interrupts the beam emitted by the IR sensor transmitter, the current stops flowing to the IR sensor receiver and the voltage drops to zero. The data logger records all drops in voltage. **B)** Electrical circuits highlighted. Each yellow box delimits the components of a circuit connected to the breadboard. Multiple electric circuits can be connected to a single breadboard in alternating rows. The size of the solderless breadboard limits how many flight cells can be accommodated.

**Figure 5: Insects of different sizes magnetically painted and tethered.** **A)** *Drosophila melanogaster* (common fruit flies) magnetically painted and tethered. Fruit flies are small insects (body length  $\leq 5$  mm; mass = 0.2 mg) that need to first be anesthetized with ice or CO<sub>2</sub> under a microscope before applying the magnetic paint to their thorax. **B)** Mismatch between insect size and magnet size. The magnet on the flight mill arm should best accommodate the size of the insect. Here the insect's field of vision is obstructed because the magnet is too large. A smaller conical magnet or magnetic strip would solve this mismatch. **C-F)** *Oncopeltus fasciatus* (milkweed bugs) and *Jadera haematoloma* (soapberry bugs) magnetically painted and tethered. Larger bugs (body length  $> 5$  mm; mass  $> 0.1$  g) can be pinched by their legs before applying a coat of paint on their thorax.

**Figure 6: Examples of WDH flight recordings.** Voltage troughs represent complete revolutions of the flight mill's arm. The red dotted lines divide the display, and the seconds-per-division (sec/div) of each panel are highlighted in blue. Black vertical lines mark the cursor time. **A)** Event markers. The sec/div was changed from 0.2 sec/div to its max, allowing the entire waveform to be drawn across the screen. All event markers taken across all channels will only be visible in the first channel as lines that run from the max voltage to the bottom of the channel field window. All event makers for this recording set are within the yellow oval. **B)** Signal loss. In another recording set, the sec/div was changed from 0.2 sec/div to 15 sec/div to help visualize a recorded signal lost from 17:09 to 17:15 in channel 3. All other channels such as channel 4 continued to function properly. **C)** Double troughs and mirror troughs. Double troughs are when the voltage dips, rises, and then quickly dips and rises again to create what appears to be two merged troughs in one beam-breaking event. The double troughs also mirror one another, which suggests that the flag moved back and forth between the sensor, which usually happens when an insect stops

flying. The Python scripts correct for each case. **D)** Voltage noise. Soon after 13:14, small bumps in the voltage can be seen, which suggest voltage noise in the recording.

**Figure 7: Representative trough diagnostic data from *Jadera haematoloma* (soapberry bug).** Potential noise or overly sensitive troughs are readily recognized in the flight recordings. **A)** An optimal, robust recording from example individual 318. There was no change in the number of troughs as the minimum and maximum deviation values increased, and so the troughs were robust enough to be identified despite a large standardization interval. **B)** A sub-optimal, but still robust recording from example individual 371. There is a drop in the number of troughs as the minimum and maximum deviation values increased; however, the drop was minimal (8 troughs). There could be noise and some sensitive troughs but nothing substantial. **C)** A noisy recording from example individual 176. There is a clear and rapid drop in the number of troughs identified as the minimum and maximum deviation values increased until its number plateaus at 12 troughs. This signals a lot of potential noise or overly sensitive troughs while the 12 troughs remain as robust troughs.

**Figure 8: Representative flight data from *Jadera haematoloma* (soapberry bug).** Four categories of flight behavior can be identified in the flight recordings. **A)** Continuous flight. This individual flew continuously for 1.67 h, beginning at high speeds and then tapering over time into lower speeds. **B)** Bursting flight. This individual flew only in bursts within the first 30 min of their trial. Bursters can reach high speed but this individual could only retain low speeds. **C)** Continuous to bursting flight. This individual had maintained continuous flight for 25 min and then tapered off into bursts for the remaining 5 min of their trial. **D)** Bursting to continuous flight. This individual began as a burster, reaching high sporadic speeds, and then transitioned into continuous flight for about 4 h.

**Figure 9: Representative channel visualization of multiple flight trials within a single recording set.** Each color represents an individual soapberry bug, *Jadera haematoloma*, at its given channel letter and channel number during its trial. All start times, stop times, and filenames were extracted from each individual's unique flight track txt file.

**Supplemental Figure 1: Kerf key.** Kerf is the thickness of the material removed or lost in the process of cutting that material. For a laser cutter, two important factors will determine the width of the kerf: the beam width and the material type. To test and calculate the exact kerf, laser cut the key and fit the 20 mm width key into the slot that it fits most securely. Then, subtract the slot width value from the key width value. For example, a key with a width of 20 mm that fits into a 19.5 mm slot will have a kerf thickness of 0.5 mm.

**Supplemental Figure 2: Flowchart of the functions and data structures of each Python script.** An overview of the inputs, functional processes, and outputs of each Python script for the proposed flight mill is summarized and described through examples.

**Supplemental Figure 3: Comparison of low sampling frequencies. A)** Relationship between voltage drop and speed by sampling frequency. Each color and shape represents a sampling

frequency (100 Hz, 75 Hz, 50 Hz, and 25 Hz). Voltage drop is synonymous with the size of the trough. Lines fit second order regressions, which describe the decrease in trough size as speed increases and the following rise in trough size at higher speeds. The shaded bar runs from 0 V to 0.1 V, which marks the voltage range in which noise occurs. Data were collected on cell B-4 using the WinDAQ recording software and with foil flag dimensions 30 mm length by 30 mm width. The flight mill arm was spun rapidly by hand and left to spin until it stopped moving. Sampling frequencies 25 Hz or lower are in danger of misidentifying troughs as noise during standardization and diagnostic tests. Sampling frequencies of 100 Hz or higher are especially robust at recording large troughs for speeds less than 1 m/s. **B)** Trough sizes of different sampling frequencies seen through the waveform. As the sampling frequencies decrease, their representation on the waveform also shrinks.

## **DISCUSSION:**

The simple, modern flight mill provides a range of advantages for researchers interested in studying the flight behavior of a model species by delivering a reliable and automated design that tests multiple insects efficiently and cost-effectively<sup>13,31,35</sup>. Likewise, there is a strong incentive for researchers to adapt to fast-emerging technologies and techniques from industry and other scientific fields to design and build experimental tools to study ecological systems<sup>9,32,33</sup>. This protocol takes advantage of two rapidly emerging technologies, the 3D printer and the laser cutter, which are becoming increasingly available in communal makerspaces, in order to enhance the simple, modern flight mill. These enhancements provide a more flexible, adjustable, and collapsible design that accommodates insects of different sizes, minimizes stress placed on the insect, and allows the flight mill to be transported easily to multiple locations or environments. Furthermore, the additional expenses of using the technologies are minimal or even free. However, these technologies can also be a challenge to experiment with if reaching proficiency in using vector graphics editors and 3D image software is not readily available. In turn, the flight mill presented here serves to both encourage researchers to incorporate available emerging technologies in their workflow and to allow researchers to build a customizable, flexible, and effective flight mill without specialized knowledge of electronics, programming, or computer-aided design (CAD) models.

The strongest aspects of this protocol are the makerspace's technologies that expand a user's flight mill design options, the use of magnetic paint to minimize insect stress, and the automation of flight recordings that processes multiple insects within a single recording. The laser cutter offers precise and exact cutting capabilities that can handle jobs of almost any complexity. The user can modify the acrylic support structure to mount additional 3D prints or purchased items. The 3D printer allows the user to create customizable flight mill components that can bypass costly, pre-made products with narrowly adjustable dimensions. 3D prints not proposed in this paper can also be built, such as landing platform, supports that can quickly exchange between magnetic bearings and ball bearings, or even a new attachment that tethers an insect. Finally, the use of automated recording software and Python scripts to differentiate multiple flight trials within a single recording makes it possible to study sporadic bouts of flight to very long bouts of flight. However, given how variable flight activity and duration is across species, it is suggested that the user conducts preliminary trials in order to understand the limits and general patterns

of a species' flight behavior so as to optimize data collection. The user can also assess the integrity of their recordings using the diagnostic heatmap(s) and can account for any necessary speed corrections in the scripts.

Researchers should also be aware of the flight mill's general constraints. Previous studies have made known and have attempted to remediate the limitations of tethered flight, including a lack of tarsal contact to allow the insect to rest at will<sup>18,31</sup>, the absence of energy expended when an insect takes-off<sup>34</sup>, the additional drag the insect overcomes when pushing the flight mill arm, and the insect needing to compensate for the outward aerodynamic forces experienced due to the centrifugal acceleration of its circular flight track<sup>6,35</sup>. Additionally, there continue to be inconsistencies on how to categorize or more precisely quantify the short or 'trivial' bursts insects display, especially when comparing the flight behavior and mechanisms of large migratory insects to those of small insects who exhibit mostly hovering flight<sup>24,36,37</sup>. Despite these limitations, there has been significant progress in capturing and categorizing flight behavior within insect species, and researchers have continued to couple the flight mill with other technologies and methods<sup>6-8</sup>.

The makerspace as a location of creativity, collaboration, and low barriers will further inspire researchers to troubleshoot 3D print design limitations or laser cut more intricate designs. Studies have surveyed the effectiveness of makerspaces not just as iterative product-making spaces but also as places of accelerated learning<sup>10-12</sup>. Engineering students overall scored higher in design comprehension, design documentation, and model quality when their designs were made using makerspace technology<sup>11</sup>. Additionally, their model development time dropped by 50%, indicating that makerspace exploration outperformed traditional rote theory and application coursework<sup>11</sup>. In turn, researchers with little design knowledge will be able to deepen it, and researchers who are also educators can take advantage of this space as a means to increase design organization, craftsmanship, and technical dexterity for students. In a discipline like ecology that already makes use of a variety of tools for field and laboratory work, researchers can also develop, share, and standardize novel or enhanced tools. The flight mill proposed in this paper is only the start of what could be an approach to democratizing and rapidly spreading new means of collecting data.

Flight mills have played an important role in enabling researchers to understand the dispersal of insects – an ecological phenomenon still essentially intractable in the field. Future advances in the design and application of the flight mill can be achieved as researchers become more proficient in emerging technologies and the software accompanying those technologies. This could include designing flight mill arm bearings that allow vertical lift or gives the insect greater flight orientation flexibility. Additionally, the precision of laser cutters and 3D printers may be necessary for researchers interested in scaling down and calibrating for small insects with mostly hovering capabilities. In turn, the goal of this protocol was to provide an easy entry to these technologies while constructing one of the most common and useful devices in the field of behavioral ecology – the flight mill. If researchers have access to a communal makerspace and are committed to navigating its technologies, the resulting enhancements and improvements of the modern flight mill will lead to creative and collaborative flight mill design and will continue

to offer insights into the underlying traits and mechanisms that influence insect species' variations and patterns in movement.

#### ACKNOWLEDGMENTS:

I would like to thank Meredith Cenzer for purchasing all flight mill materials and providing continuous feedback from the construction to the write-up of the project. I also thank Ana Silberg for her contributions to standardize\_troughs.py. Finally, I thank the Media Arts, Data, and Design Center (MADD) at the University of Chicago for permission to use its communal makerspace equipment, technology, and supplies free of charge.

#### DISCLOSURES:

The author has nothing to disclose.

#### REFERENCES:

1. Krogh, A., Weis-Fogh, T. Roundabout for studying sustained flight of locusts. *Journal of Experimental Biology*. **29**, 211-219 (1952).
2. Hocking, B. The intrinsic range and speed of flight of insects. *Transactions of the Royal Entomological Society of London*. **104** (8), 223-345 (1953).
3. Chambers, D. L., O'Connell, T. B. A flight mill for studies with the mexican fruit fly. *Annals of the Entomological Society of America*. **62** (4), 917-920 (1969).
4. Chambers, D. L., Sharp, J. L., Ashley, T. R. Tethered insect flight: A system for automated data processing of behavioral events. *Behavior Research Methods & Instrumentation*. **8** (4), 352-356 (1976).
5. Naranjo, S. E. Assessing insect flight behavior in the laboratory: a primer on flight mill methodology and what can be learned. *Annals of the Entomological Society of America*. **112** (3), 18-199 (2019).
6. Ribak G., Barkan S., Soroker V. The aerodynamics of flight in an insect flight-mill. *PLoS ONE*. **12** (11), e0186441 (2017).
7. Pollack G.S., Martins, R. Flight and hearing: ultrasound sensitivity differs between flight-capable and flight-incapable morphs of a wing-dimorphic cricket species. *The Journal of Experimental Biology*, **210**, 3160-3164 (2007).
8. Koehler, C., Liang, Z., Gaston, Z., Wan, H., Dong, H. 3D reconstruction and analysis of wing deformation in free-flying dragonflies. *The Journal of Experimental Biology*. **215**, 3018-3027 (2012).
9. Behm, J. E., Waite, B. R., Hsieh, S. T., Helmus, M. R. Benefits and limitations of three-dimensional printing technology for ecological research. *BMC Ecology*. **18**, 1-13 (2018).
10. Sheridan, K. M., et al. Learning in the making: A comparative case study of three makerspaces. *Harvard Educational Review*. **84**, 505-531 (2014).
11. Khalifa, S., Brahimi, T. Makerspace: A novel approach to creative learning. *Institute of Electrical and Electronics Engineers Xplore*. **1**, 43-48 (2017).
12. Smay, D., Walker, C. Makerspaces: A creative approach to education. *Teacher Librarian*. **42**, 39-43 (2015).
13. Attisano, A., Murphy, J. T., Vickers, A., Moore, P. J. A simple flight mill for the study of tethered flight in insects. *Journal of Visualized Experiments*. **106**, e53377 (2015).



14. Reynolds, D. R., Riley, J. R. Remote-sensing, telemetric and computer-based technologies for investigating insect movement: a survey of existing and potential techniques. *Computers and Electronics in Agriculture*. **35** (2-3), 271-307 (2002).
15. Davis, M. A. Geographic patterns in the flight ability of a monophagous beetle. *Oecologia*. **69**, 407-412 (1986).
16. Taylor, R. A. J., Bauer, L. S., Poland, T. M., Windell, K. N. Flight performance of *Agrilus planipennis* (Coleoptera: Buprestidae) on a flight mill and in free flight. *Journal of Insect Behavior*. **23**, 128-148 (2010).
17. Irvin, N. A., Hoddle, M.S. Assessing the flight capabilities of fed and starved *Allograpta obliqua* (Diptera: Syrphidae), a natural enemy of Asian citrus psyllid, with computerized flight mills. *Florida Entomologist*. **103** (1), 139-140 (2020).
18. Minter, M. et al. The tethered flight technique as a tool for studying life-history strategies associated with migration in insects. *Ecological Entomology*. **43** (4), 397-411 (2018).
19. Dingle, H., Blakley, N. R. Miller, E. R. Variation in body size and flight performance in milkweed bugs (*Oncopeltus*). *Evolution*. **34** (2), 371-385 (1980).
20. Martini X., Hoyte, A., Stelinski, L. L. Abdominal color of the Asian citrus psyllid (Hemiptera: Liviidae) is associated with flight capabilities. *Annals of the Entomological Society of America*. **107** (4), 842-847 (2014).
21. Chen, M. et al. Flight capacity of *Bactrocera dorsalis* (Diptera: Tephritidae) adult females based on flight mill studies and flight muscle ultrastructure. *Journal of Insect Science*. **15** (1), 141 (2015).
22. Guo, J., Li, X., Shen, X., Wang, M., Wu, K. Flight performance of *Mamestra brassicae* (Lepidoptera: Noctuidae) under different biotic and abiotic conditions. *Journal of Insect Science*. **20** (1), 1-9 (2020).
23. Johnson, M. W., Toscano, N. C., Jones, V. P., Bailey, J. B. Modified ultrasonic actograph for monitoring activity of lepidopterous larvae. *Proceedings of the Hawaiian Entomological Society*. **27**, 141-146 (1986).
24. Cheng, X., Sun, MA. Wing-kinematics measurement and aerodynamics in a small insect in hovering flight. *Scientific Reports*. **6**, 25706 (2016).
25. Holland, J.D. Dispersal kernel determines symmetry of spread and geographical range for an insect. *International Journal of Ecology*. **2009**, 4 (2009).
26. Frouz, J. Kindlmann, P. Source-sink colonization as a possible strategy of insects living in temporary habitats. *PLoS ONE*. **10** (6), 1-10 (2015).
27. Ventola, C. L. Medical applications for 3D printing: Current and projected uses. *Pharmacy & Therapeutics*. **39** (10), 704-711 (2014).
28. Martí-Campoy, A., et al. Design of a computerized flight mill device to measure the flight potential of different insects. *Sensors (Basel)*. **16** (4), 1-21 (2016).
29. Dubois, G. F., Vernon, P., Brustel, H. A flight mill for large beetles such as *Osmoderma eremita* (Coleoptera: Cetoniidae). *Saproxyllic Beetles. Their Role and Diversity in European Woodland and Tree Habitats*. **14**, 219-224 (2009).
30. Webster, M. N., Doner, J. P., Wikstrom, V., Lugt, P. Grease degradation in R0F bearing tests. *Tribology Transactions*. **50** (2), 187-197 (2007).

- 870 31. Jones, H. B. C., Lim K. S., Bell, J. R., Hill, J. K., Chapman, J. W. Quantifying interspecific  
871 variation in dispersal ability of noctuid moths using an advanced tethered flight technique.  
872 *Ecology and Evolution*. **6** (1), 181-190 (2016).
- 873 32. Walker, M., Humphries, S. 3D Printing: applications in evolution and ecology. *Ecology and*  
874 *Evolution*. **9** (7), 4289-4301 (2019).
- 875 33. Shahrubudin, N., Lee, T. C., Ramlan, R. An overview of 3D printing technology:  
876 technological, materials, and applications. *Science Direct*. **35**, 1286-1296 (2019).
- 877 34. Taylor, R. A. J., Nault, L. R., Styer, W. E., Cheng, Z. B. Computer-monitored, 16-channel  
878 flight mill for recording the flight of leafhoppers (Homoptera: Auchenorrhyncha). **85** (5), 627-632  
879 (1992).
- 880 35. Nachtigall, W., Hanauer-Thieser, U., Mörz, M. Flight of the honey bee VII: metabolic  
881 power versus flight speed relation. *Journal of Comparative Physiology B*. **165**, 484-489 (1995).
- 882 36. Hardie, J. Flight behavior in migrating insects. *Journal of Agricultural Entomology*. **10** (4),  
883 239-245 (1993).
- 884 37. Blackmer, J. L., Naranjo, S. E., Williams, L. H. Tethered and untethered flight by *Lyrgus*  
885 *Hesperus* and *Lygus lineolaris* (Heteroptera: Miridae). *Environmental Entomology*. **33** (5), 1389-  
886 1400 (2004).

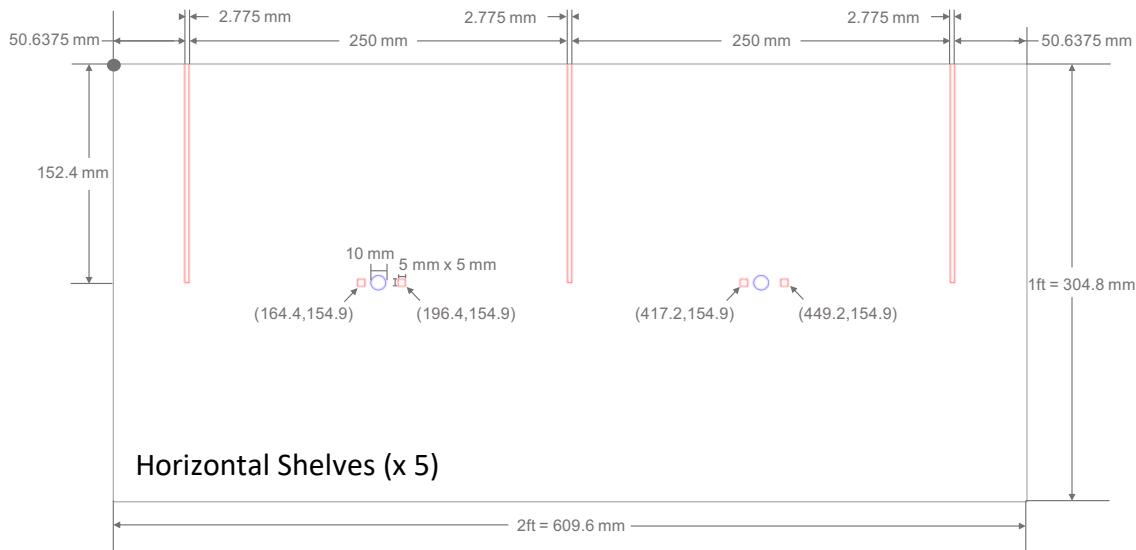
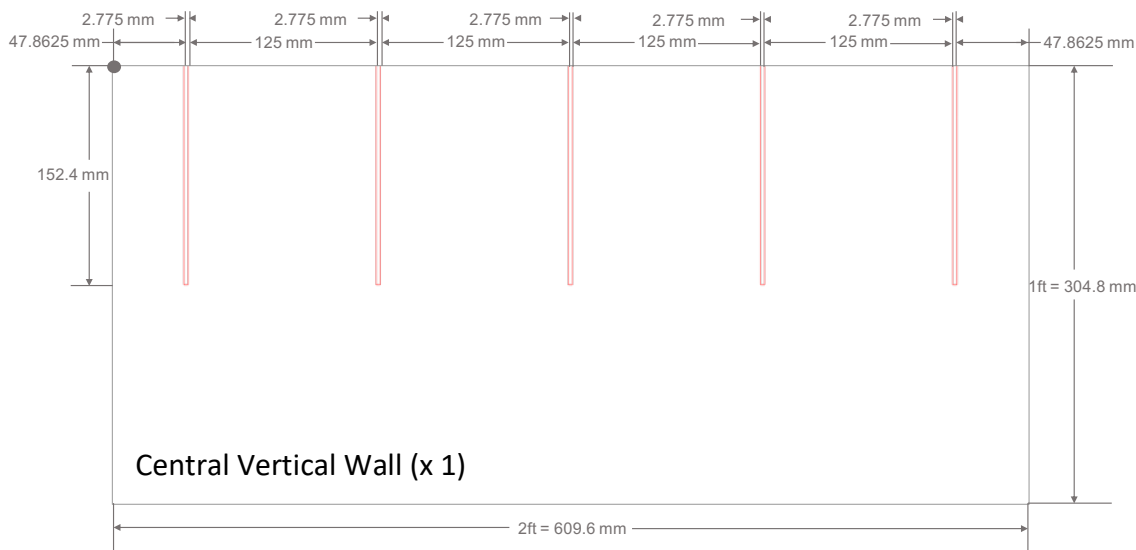
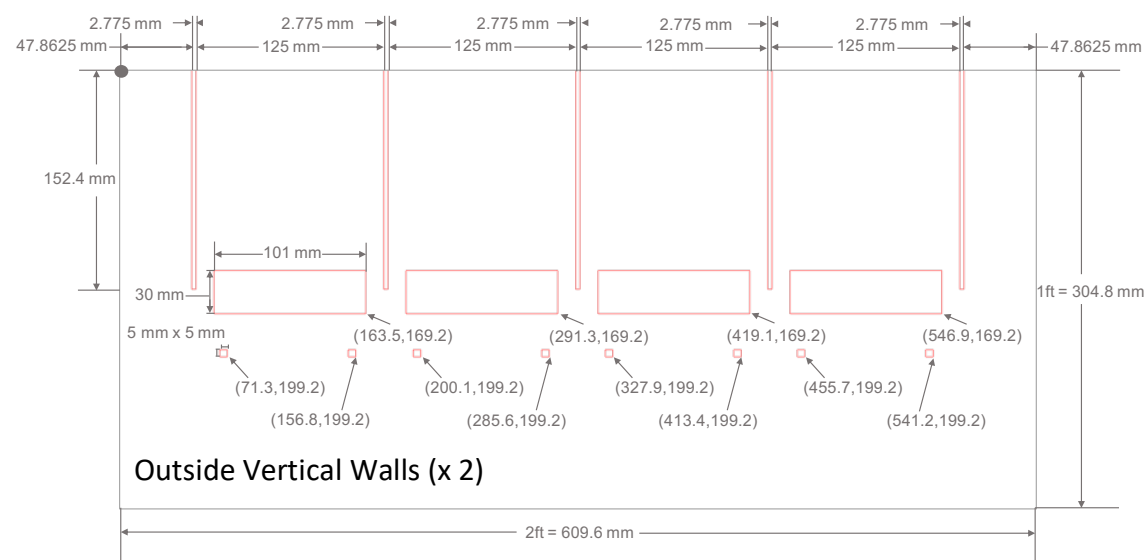


Figure 2

[Click here to access/download/Figure/F2\\_flight\\_mill.pdf](#)

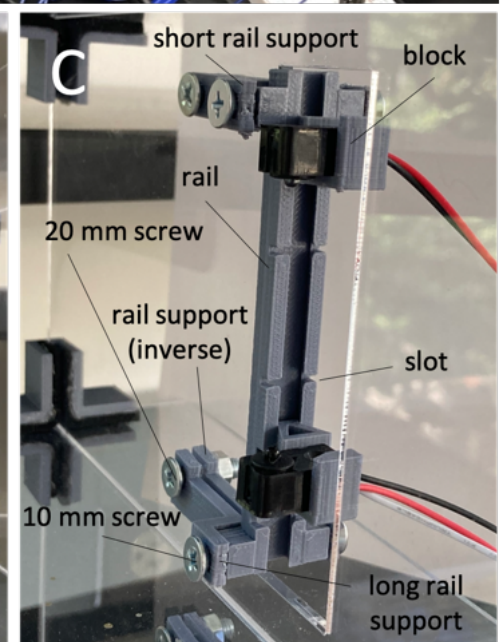
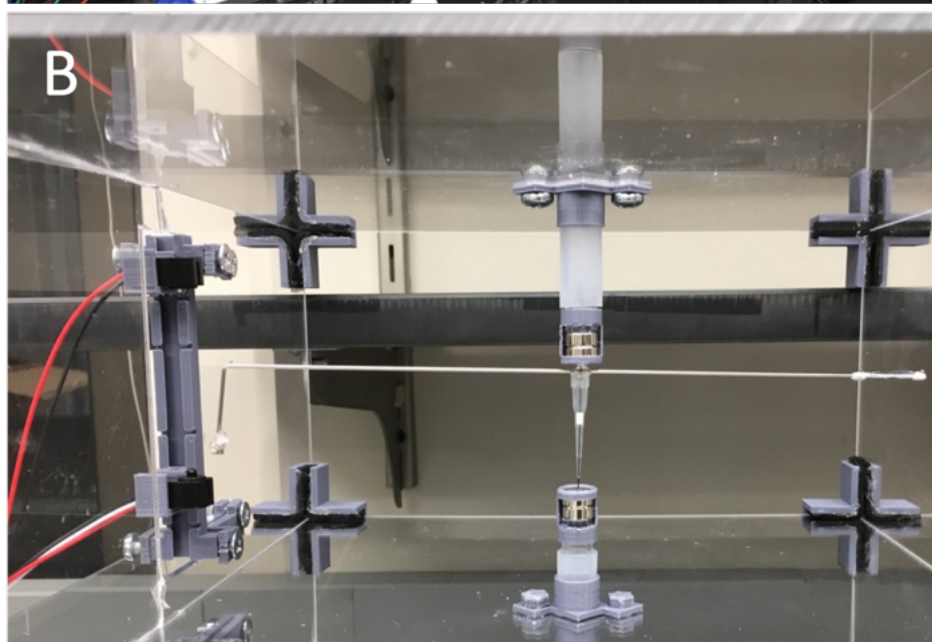
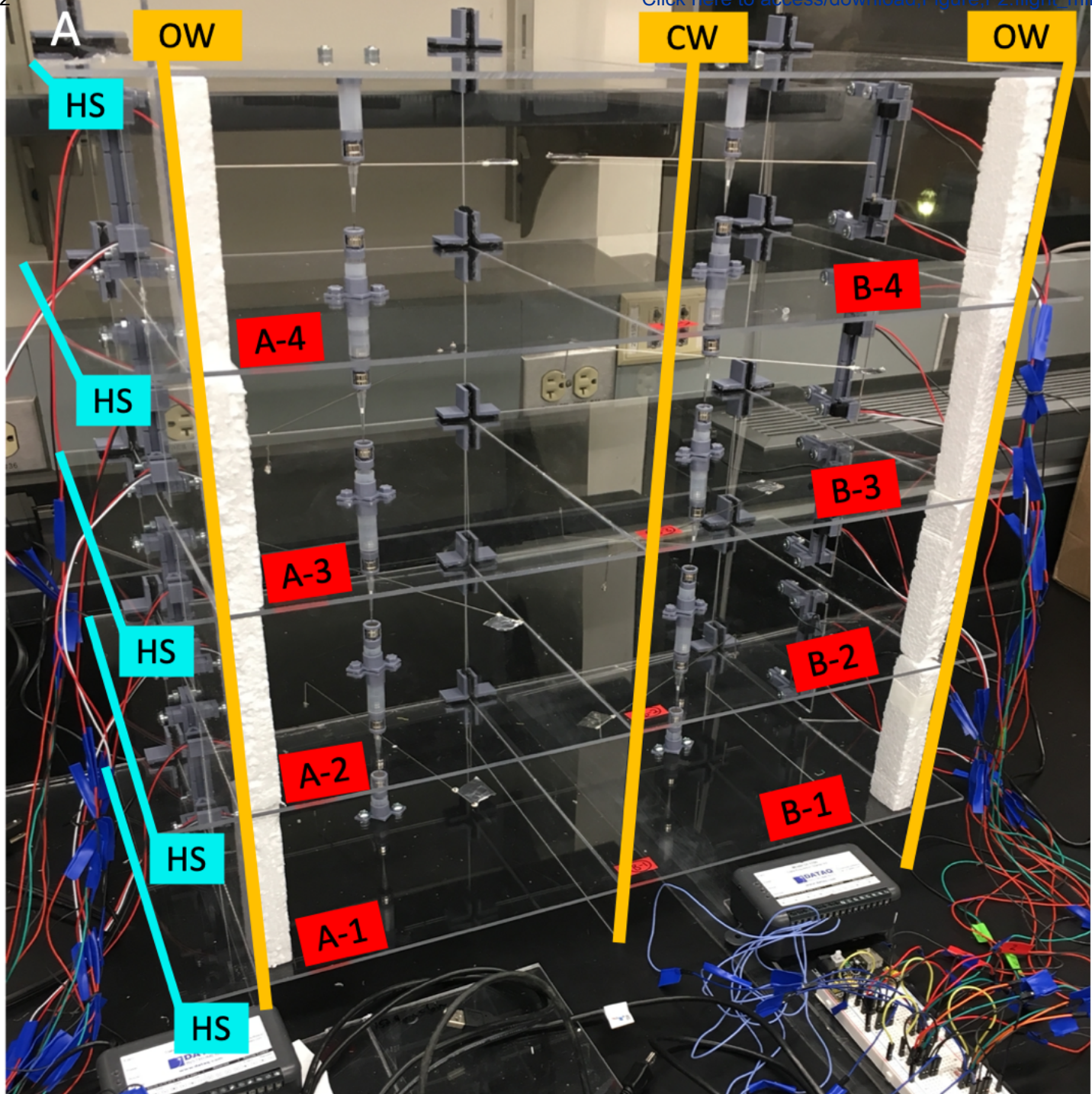




Figure 3

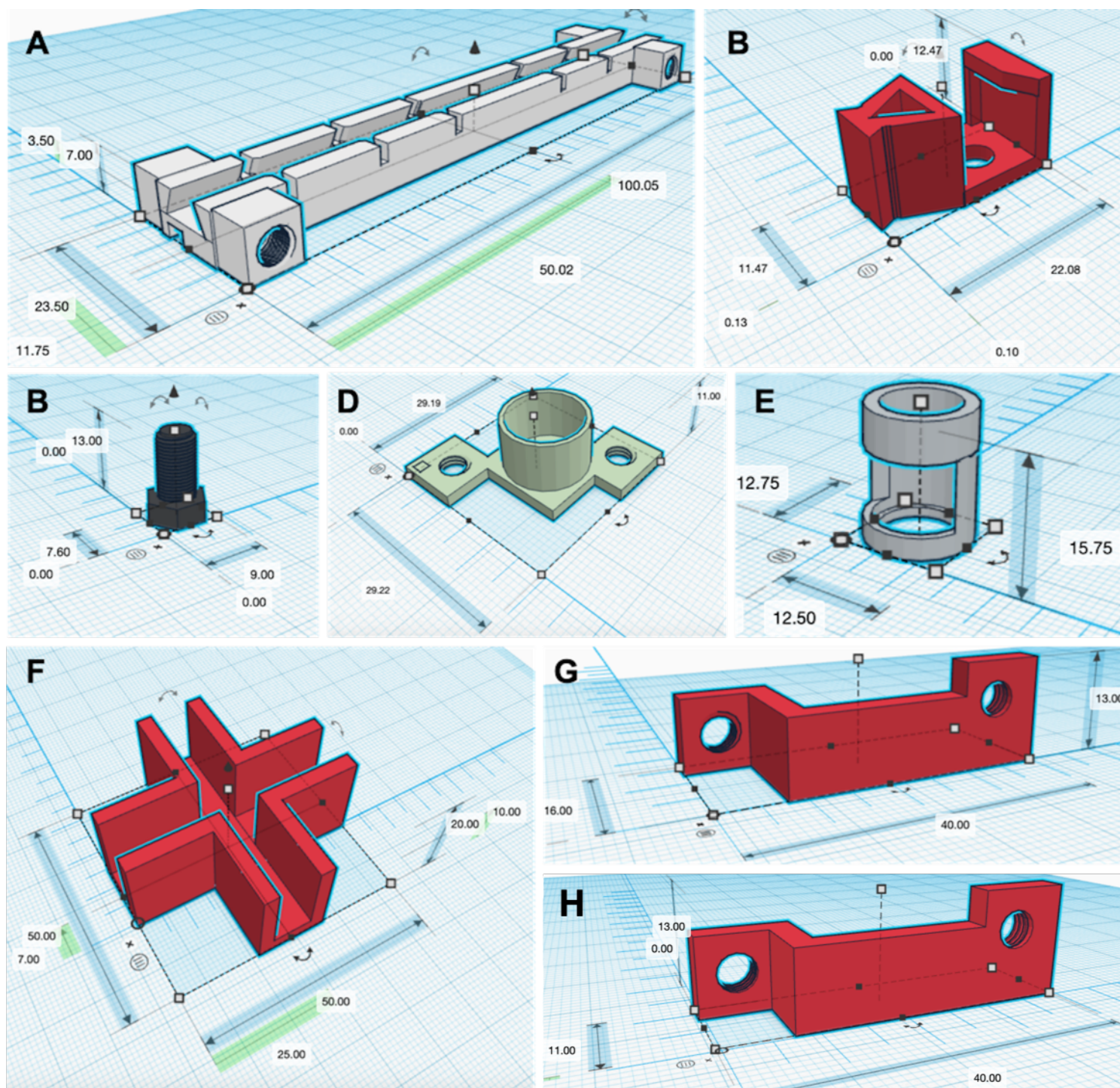




Figure 4

[Click here to access/download;Figure;F4.circuit.pdf](#)

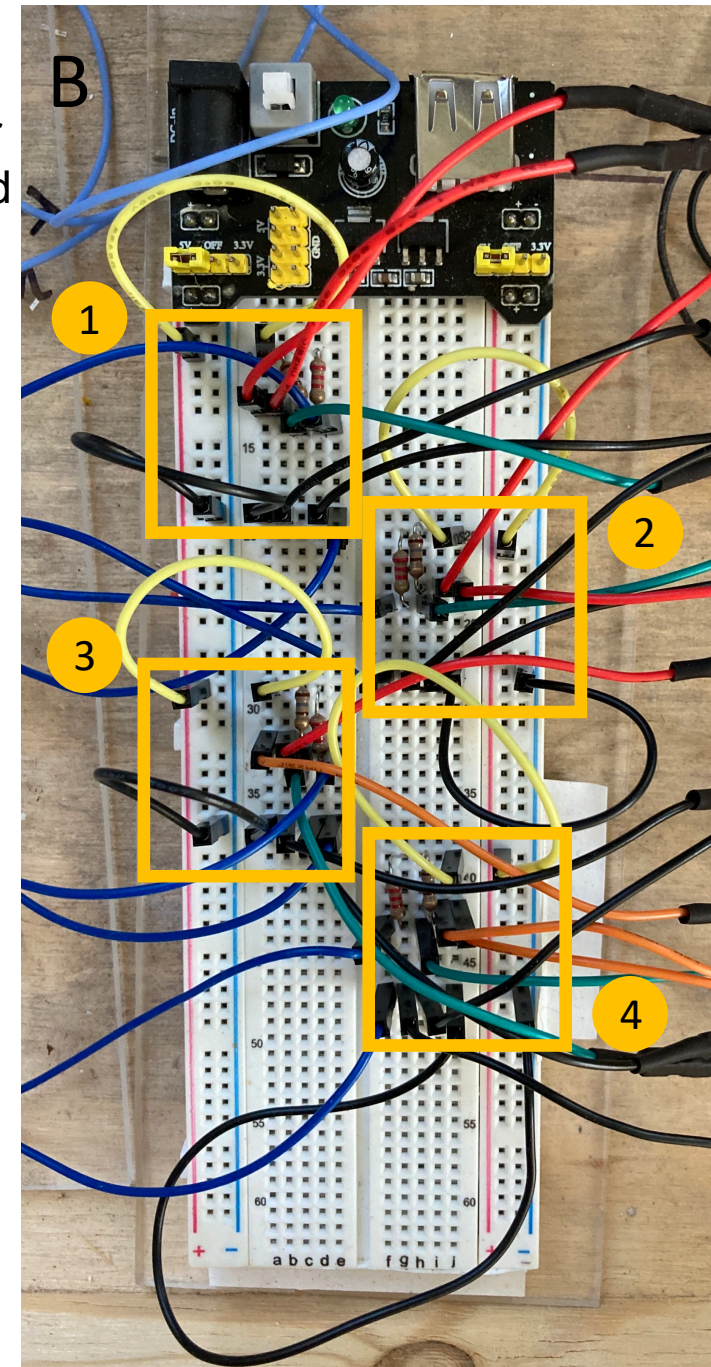
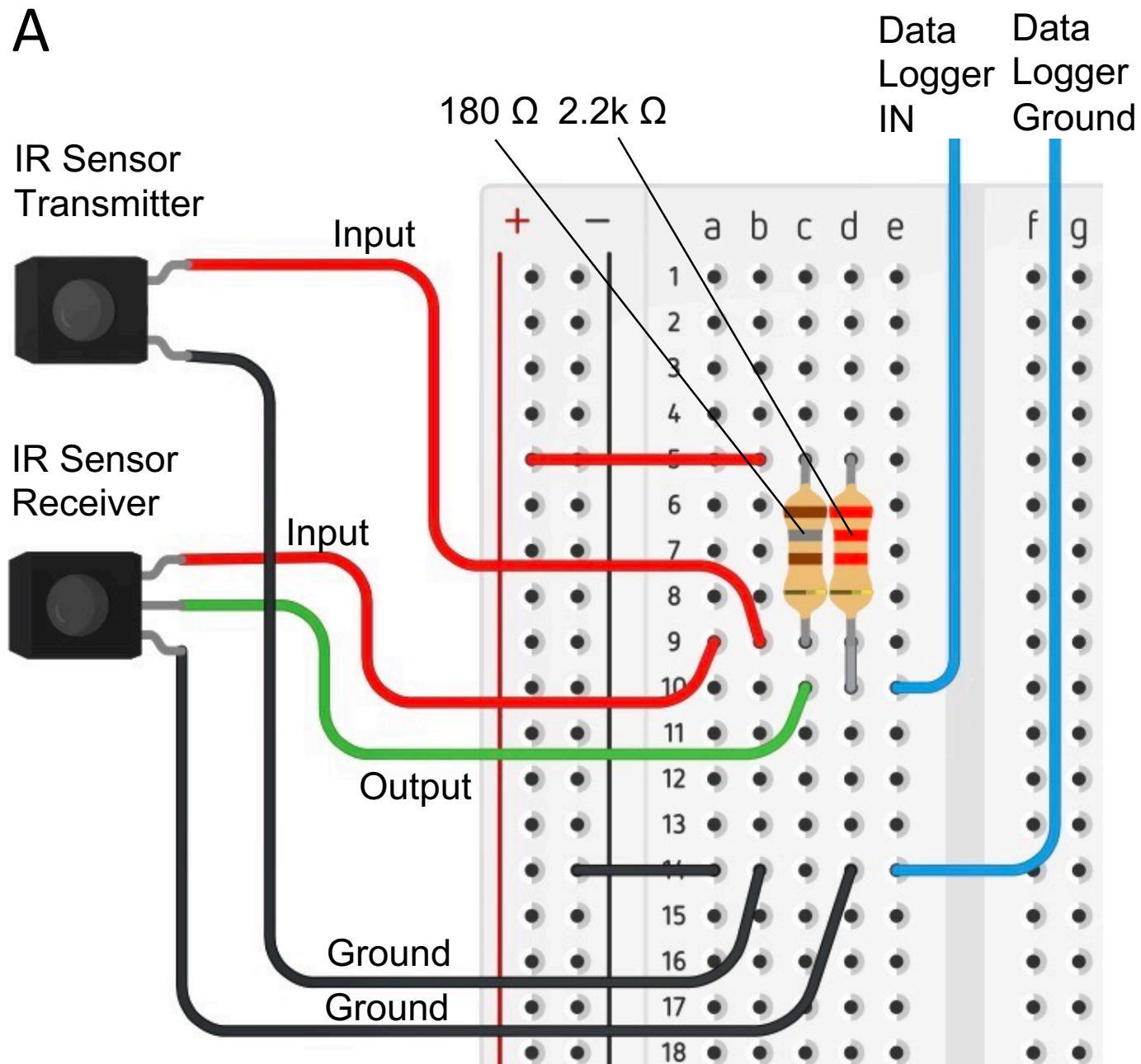




Figure 5

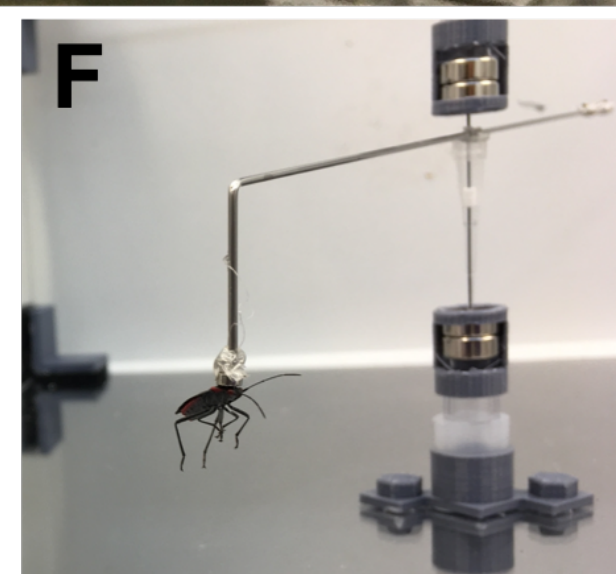
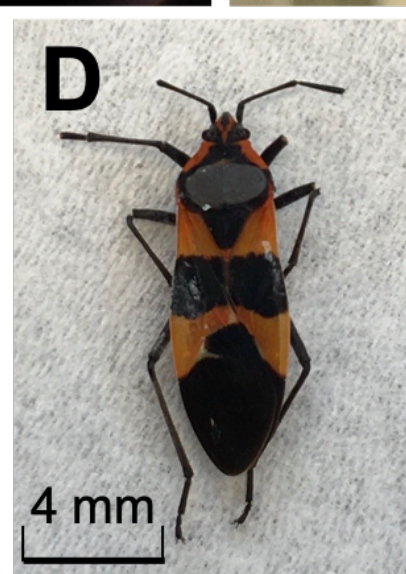
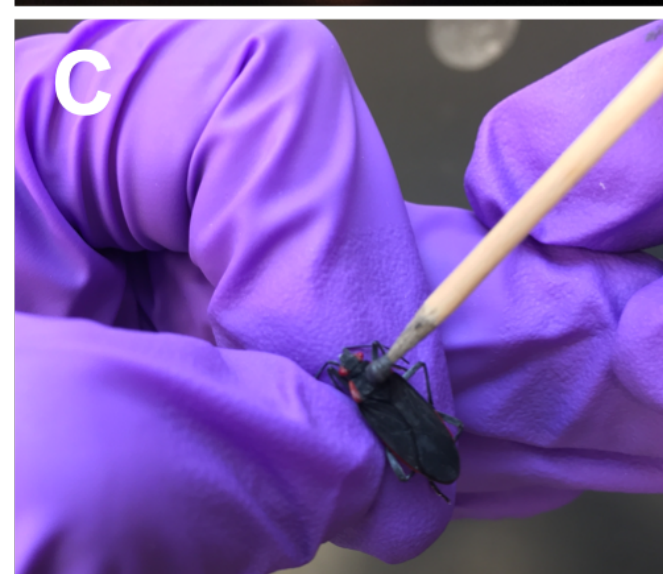
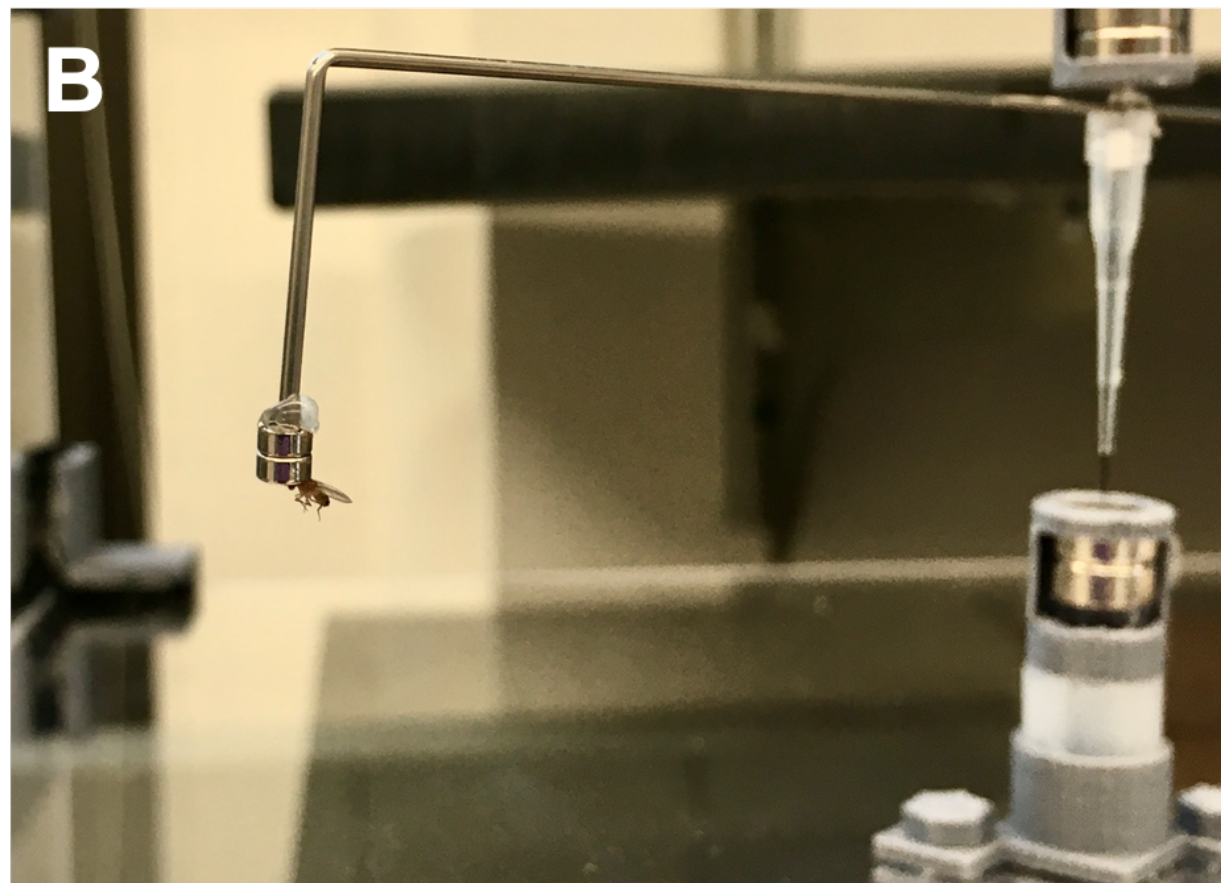
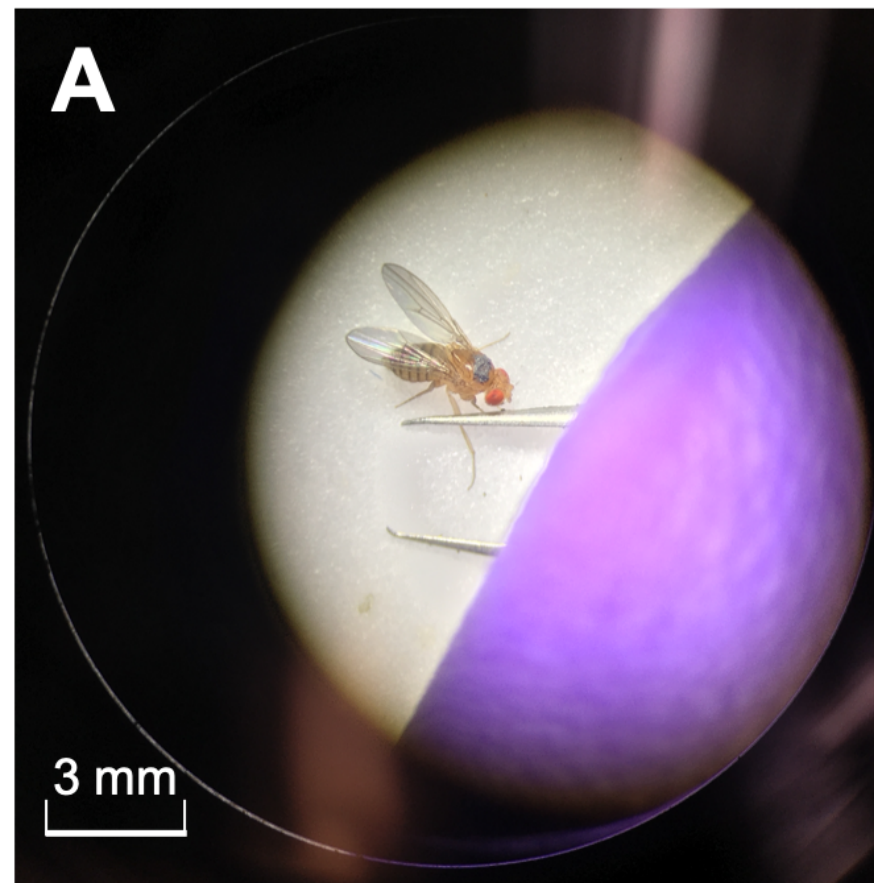


Figure 6

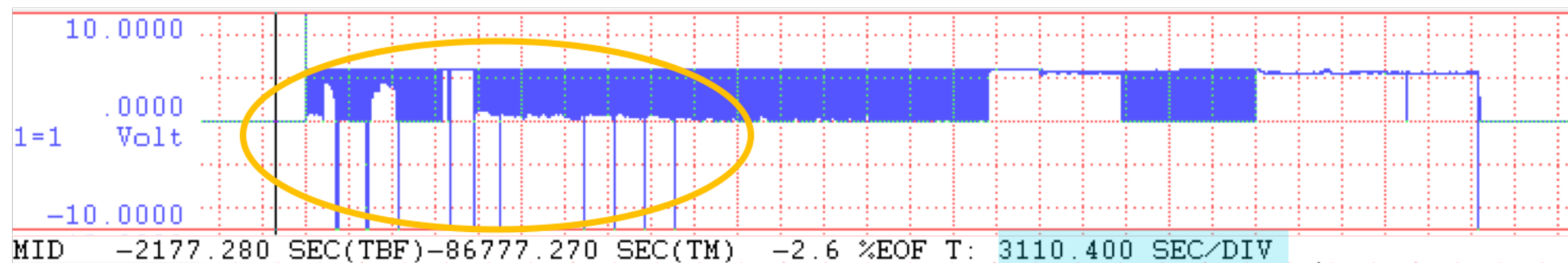
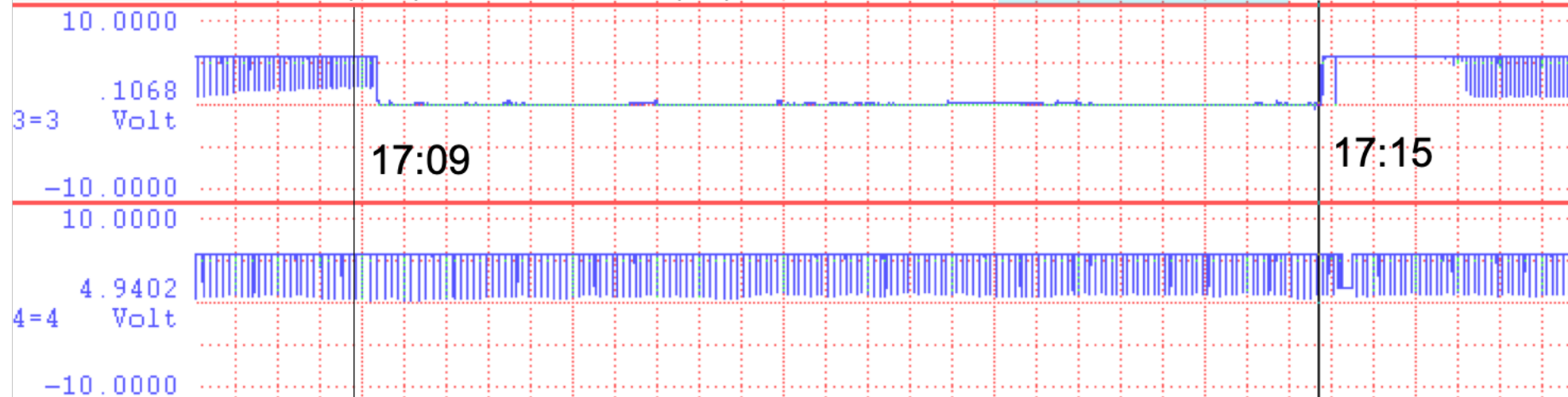
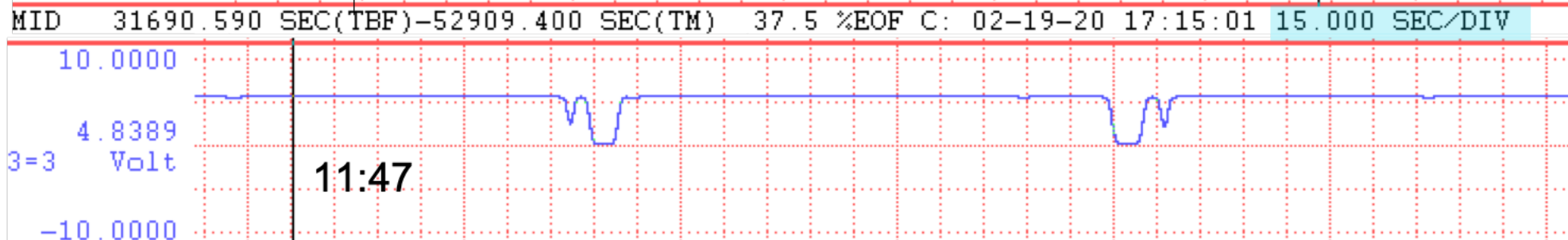
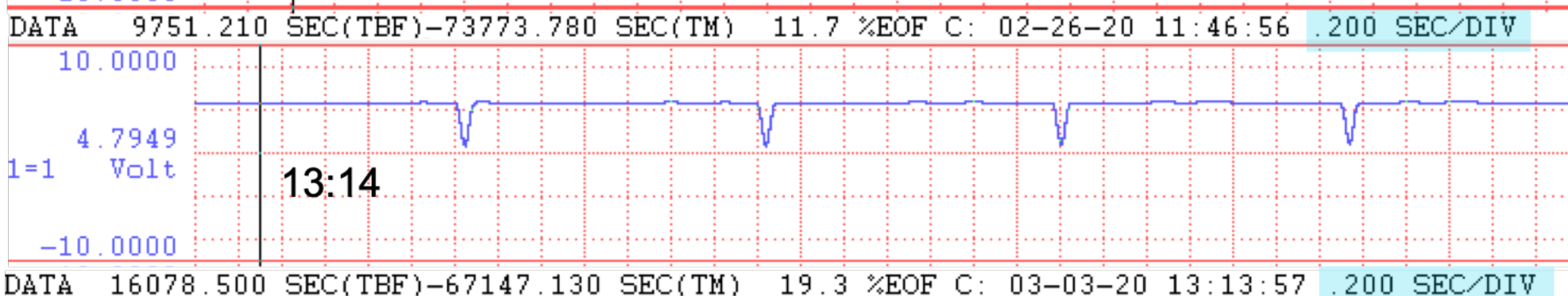
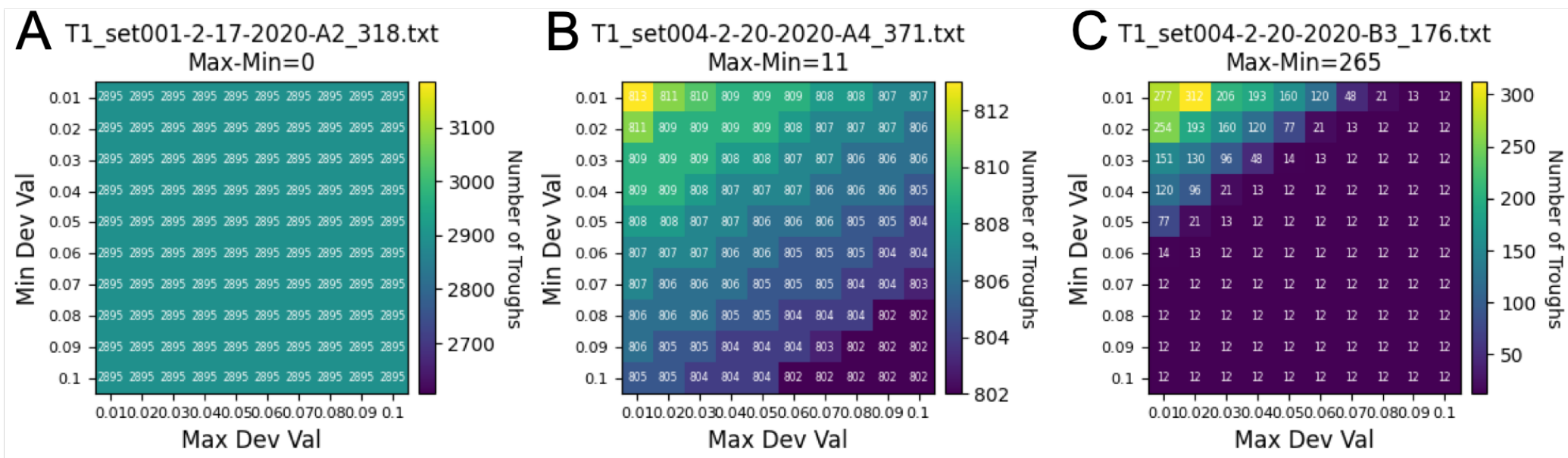
**A****B****C****D**



Figure 7



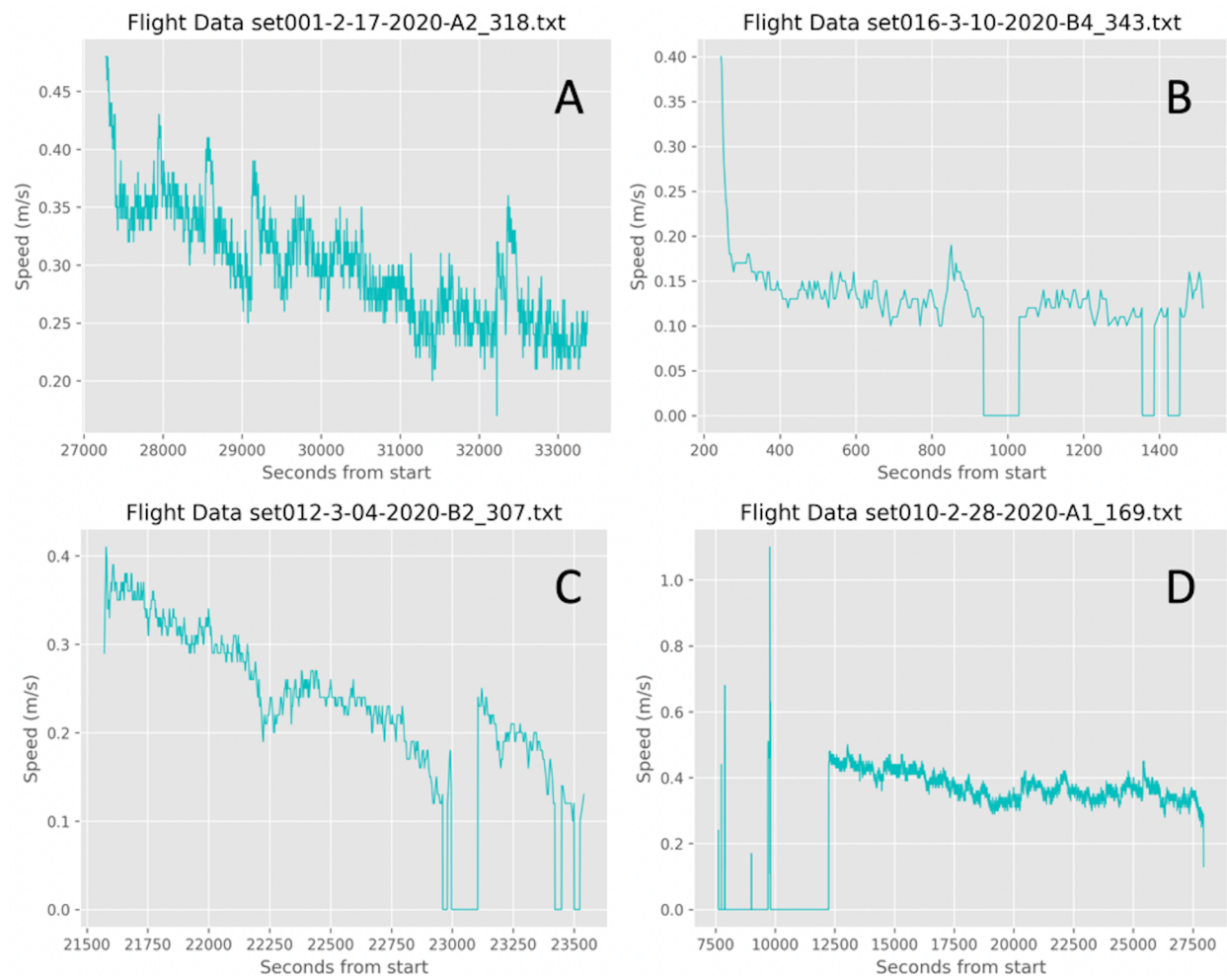
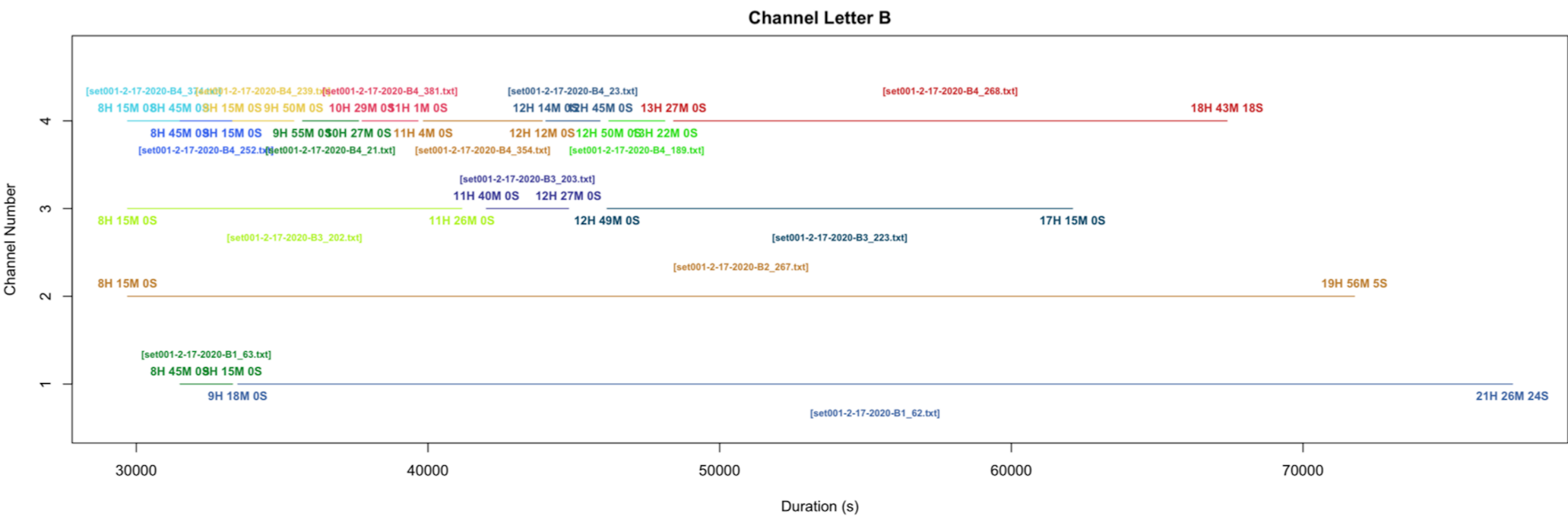


Figure 9



Name	Company	Catalog Number
180 $\Omega$ Resistor	E-Projects	10EP514180R
19 Gauge Non-Magnetic Hypodermic Steel	MicroGroup	304H19RW
2.2 k $\Omega$ Resistor	Adafruit	2782
3D Printer	FlashForge	700355100638
3D Printer Filament	FlashForge	PLA-1KG
3D Printing Slicing Software	FlashPrint	4.4.0
Acrylic Plastic Sheets	Blick Art Supplies	28945-1006
Aluminum Foil	Target	253-01-0860
Breadboard Power Supply	HandsOn Tech	MDU1025
DI-1100 USB Data Logger	DATAQ Instruments	DI-1100
Electrical Wires	Striveday	B077HWS5XV
Entomological Pins	BioQuip	1208S2
Filtered 20 $\mu$ L Pipette Tip	Fisher Scientific	21-402-550
Hot Glue Gun with Hot Glue	Joann Fabrics	17366956
IR Sensor	Adafruit	2167
Large Clear Vinyl Tubing	Home Depot	T10007008
Large Magnets	Bunting	EP654
Laser Cutter	Universal Laser Systems	PLS6.75
M5 Hex Nut	Home Depot	204274112
M5 Long Iron Screws	Home Depot	204283784
M5 Short Iron Screws	Home Depot	203540129
Neoprene Rubber Sheet	Grainger	60DC16
Power Adaptor	Adafruit	63
Small Clear Vinyl Tubing	Home Depot	T10007005
Small Magnets	Bunting	N42P120060
Solderless MB-102 Breadboard	Adafruit	239
Sophisticated Finishes Iron Metallic Surfacers	Blick Art Supplies	27105-2584
Wire Cutters	Target	84-031W

## Comments

Carbon film; stiff 24 gauge lead.

Carbon film; stiff 24 gauge lead.

Diameter 1.75 mm; 1kg/roll.

Can take 6.5V to 12V input and can produce 3.3V and 5V.

Has 4 differential armored analog inputs.

24 gauge solid wire.

Size 2; diameter 0.45 mm.

This is the 3 mm IR version; works up to 25 cm.

Inner diameter 3/8 in; outer diameter 1/2 in; length 20 ft.

Low-friction N42 neodymium; diameter 0.394 in; length 0.157 in; holding force

Thread pitch 0.8 mm; screw length 20 mm; diameter 5 mm.

Philips pan head; thread pitch 0.8 mm; screw length 20 mm; diameter 5 mm.

Philips pan head; thread pitch 0.8 mm; screw length 10 mm; diameter 5 mm.

Length 12 in; width 12 in; depth 1/8in.

9 VDC 1000mA regulated switching; input voltage DC 3.3V 5V.

Inner diameter 1/4 in; outer diameter 3/8 in; 20 ft long.

Low-friction N42 neodymium; diameter 0.120 in; length 0.060 in; holding force

830 tie points; length 17 cm; width 5.5 cm; input voltage, DC 3.3 V 5 V.

To Dr. Vidhya Iyer and the four anonymous reviewers:

Thank you for all of your productive comments. I truly appreciated the diversity and depth of your questions. I have addressed each comment and believe it has resulted in dramatic improvements to this manuscript. I summarize the major changes I made below, and then I address each individual comment.

Major changes:

1. In the introduction and discussion, I have added new paragraphs that describe the educational and research benefits of makerspaces.
2. I have revised and added new figures. Figure 5 shows how to apply magnetic paint on insects of different sizes and how to (and how not to) tether them. Figure 7 showed line graphs before but it now shows heatmaps for the trough diagnostics. Supplemental Figure 2 shows a comprehensive flowchart of the main functions and data structures of each Python script. Supplemental Figure 3 shows a comparison between low sampling frequencies in order to help users decide which sampling frequency is best for their experiments.
3. I have corrected for grammar, SI units, and abbreviations as well as formatted references and figures to match submission guidelines.
4. I have added additional specifics on the IR sensors, masses of moving parts, dimensions of the foil flag or 3D prints, and experimental setup.
5. I have added new reference material based on reviewers' insightful recommendations. This has included four papers on the benefits of makerspaces, three papers on ball bearings, and two papers on dispersal theory and application.

Individual comments (reviews in italics; responses in plain text):

#####

*Editor:*

1. *Please take this opportunity to thoroughly proofread the manuscript to ensure that there are no spelling or grammar issues.*

Improved.

2. *Please revise the following lines to avoid previously published work: 74-75, 250-259*

Revised.

3. *Please revise the title for conciseness. "Benefits of Makerspaces" can be removed.*

I removed "Benefits of Makerspaces" from the title, but I wonder if readers would want to know where the enhancements of the machine can be primarily built. Readers could build their flight

mill in other contexts if that context also has the available technology, but the makerspace is unique and versatile as a space of creation.

4. *Please refrain from using personal pronouns: I, we, etc.*

I removed and rephrased all appearances of personal pronouns, except in the Acknowledgements. Please let me know if the Acknowledgements section needs to be revised.

5. *Please define all abbreviations before use (3D, IR, RGB).*

Corrected.

6. *JoVE cannot publish manuscripts containing commercial language. This includes trademark symbols (™), registered symbols (®), and company names before an instrument or reagent. Please remove all commercial language from your manuscript and use generic terms instead. All commercial products should be sufficiently referenced in the Table of Materials (e.g., Universal Laser Systems, FlashPrint, FlashForge, Finder 3D Printer,)*

References to commercial products in the manuscript have been removed. Readers will instead reference the Table of Materials if curious about which specific products the manuscript was modeled by.

7. *Line 170-175: Please include the specifications for the linear guide rails, linear guide rail blocks, screws, cross brackets, magnet holders, tube supports, guide rail supports, etc.*

I added dimensions (i.e. length x width x depth) for each 3D printed design in step 1.2.3. To see nuanced details of the designs, readers can view Figure 3. Otherwise, please let me know whether these are sufficient specifications.

8. *Please use standard abbreviations for SI units throughout the protocol. Examples: 10 min, 5 h.*

Corrected.

9. *Please name and specify the supplementary files used throughout the manuscript: Supplementary File in line 131.*

Corrected.

10. *Step 2: Please specify the insect used in the protocol. This data is on line 459. Please move it up to the protocol so we can include this information in the filming.*

I now mention *Jadera haematoloma* (soapberry bug) in step 2.1.1.

11. *Please consider moving Discussion of figures from the figure legends to Representative Results (Figure legend 6).*

Revised. Also, what was once Figure 6 is now Figure 7, and it shows heatmaps instead of line graphs.

12. *Figure 4: Please define the yellow boxes in the Figure legends.*

I added this definition.

13. *Please sort the table of materials in alphabetical order.*

Sorted.

#####

*Reviewer #1:*

*1. The literature review for this paper seems to be not very comprehensive. The reviewer recommends citing and discussing recently-published peer-reviewed documents related to make movement and the positive impact of makerspaces in education. Documents listed below can be considered relevant (or other relevant documents based on the author's judgment:*

*<https://search.proquest.com/docview/1774311185?pq-origsite=gscholar&fromopenview=true>  
<https://www.mdpi.com/2227-7102/10/1/8>*

*Makeology: Makerspaces as Learning Environments (Volume 1), Volume 1*

I appreciated this comment and enjoyed reading literature on the maker movement. I included more information on the many impacts of makerspaces in the introduction and discussion.

*2. Parts of this paper (Sections 1-3) does not follow the format of a peer-reviewed publication, and looks like a experimental manual. The reviewer feels that these parts need to be rewritten in the format of a paper by adding more introductory and analyzing paragraphs and removing the details of experiments.*

In response to this and another reviewer's comment, I added more analysis about the benefits and disadvantages of the flight mill I constructed and of alternative flight mills. I also removed extraneous details of the experiments in the Discussion, but, in response to other reviewers, added more pertinent experimental details.

*3. Results in some of the figures of this paper are not discussed properly. A good technique to use for figures and tables is sandwiching where the figure or table is introduced in the text, and is fully discussed after the figure or table. I recommend adding analyzing comments for the figures.*

I added more comments that aligned with the new figures and new figure edits, but I would also like to hear more about where an analyzing comment goes. When is it best for analyses to be embedded in text and when in figures?



*4. Figures need proper caption.*

I added a short title and short description for each panel in each figure where it was omitted before. This included Fig 2C, Fig 4A, Fig 4B, Fig 6A, Fig 6B, Fig 8A, Fig 8B, Fig 8C, and Fig 8D.

*5. Does the comments at the end of the paper add any important practical value to the paper? I feel they can be removed.*

I cut extraneous comment descriptions and retained comments that I thought would be most useful for a first time user of electrical/mechanical tools/equipment.

*6. I recommend putting the list of the material in the format of a table.*

Converted to CSV file now.

*7. Coding files have been provided as supplementary material. I feel the author can add pseudocode(s) or flowchart(s) for these codes in the paper.*

I added a pseudocode/flowchart for the code (Supplemental Figure 2), but I still left it as supplementary material because there was a lot to distill into one diagram. It could be distilled even further if reviewers want a more representational (not supplementary) figure in the paper.

*8. There seems to be some punctuation, grammar, and formatting errors in the paper. Please proofread and comply by the template's format.*

Revised.

*9. Figures 4, 5, 8, and supplementary figure 1 can be resized. They seem to be unnecessarily big.*

Revised.

*10. Can the author add couple of paragraphs on the effectiveness of the makerspace for education purpose. Are there any surveys or results that show the effectiveness of this work?*

I added new paragraphs in the introduction and discussion explaining survey results and course results on how effective makerspaces are in the classroom.

#####

*Reviewer #2:*

*1. L131. It is a good idea to add a kerf key.*

Agreed. Laser kerf is especially variable, and kerf keys help users see exactly which laser settings work best for the construction of major designs. Without knowing precise settings, you are very likely to underestimate or, worse, overestimate the size of holes in a design, which will end up removing too much material for the building material to be constructible or correctable anymore. This wastes a lot of useful building material that was meant to be used for the main project.

*2. Fig 1. Could you add the location of the square and rectangular holes on the Outside Vertical Wall, as well as the location of the holes on the Horizontal Shelves?*

Good question - I added a vertex coordinate for each hole in the Outside Vertical Wall and Horizontal Shelf designs. For greater figure legibility, I did not include units in the coordinates but defined the units in the figure description. Please let me know if the units need to be included in the figures. Additionally, I marked an origin for each design and updated its corresponding figure description to match the designs.

*3. Fig 3. L534. Is not H the mirror of G?*

It looks like it but it is not. H is a short linear guide rail support (11.00 mm width) and G is a long linear guide rail support (16.00 mm width) because of their different widths. However, this image is confusing because each rail support rests on a different side of the acrylic wall. H rests on the outside of the acrylic wall and G rests on the inside. To avoid this confusion, I now show the same-sided version of each support and specify between 'short' and 'long' support in the figure description.

*4. L173 and L237. What is the difference between short and long linear guide rail support? If they refer to designs G and H, maybe use 'linear guide rail support 1' and 'linear guide rail support 2'.*

See response to third question above on clarifying rail supports. I did not take up this suggestion, but potentially renaming the shorter linear guide rail, 'linear guide rail support 1', and the wider linear guide rail, 'linear guide rail support 2' is still a good idea. I left the names descriptive so they can hint to users what the difference between the rail supports is.

*5. In the case of first-time users of 3D printing, it would to add that it is possible to print several parts at the same time if they fit on the build area.*

Valuable suggestion - I added a note for first-time users at step 1.2.2. This will not only help first-time users customize their .STL files early on to help them save time, but it will also help them foresee potential pitfalls in rotating designs along the z-axis.

*6. L214-215. The horizontal shelves have to be put in the correct position so the holes are aligned.*

Also important – I added a new sentence in step 1.1.8. that tells users, during the assembly of the acrylic support structure, to make sure that the holes between horizontal shelves are aligned.

7. L242-244. *Good idea!*

Thank you!

8. L291. *As one of the strongest aspects of the protocol (L604), it would be informative to have a picture of the mill with an insect tethered with magnetic paint in order to have an idea of how it differs from gluing.*

I added a new figure (Figure 5) that shows how to apply the paint to insects of different sizes.

9. Fig 5. *Why are all the event markers of all channels displayed in channel 1? Is there any benefit of this method instead of displaying the event markers in their corresponding channel?*

Rather than a benefit, it is a limitation by the WinDAQ software. As far as I know and after trying multiple tools on the software, there is no way to attach event markers to their corresponding channel. Additionally, I found no way to export the data with a column that identifies which channel the event marker was made. I found a way around that by recording ID and channel number by hand and writing the split\_files.py script, but I would also love to put those event markers directly into the corresponding channel.

10. L546. *There should be the time scale on the horizontal axis.*

I decided against a *direct* time scale on the horizontal axis. By that I mean, I did not label each division with its time, but trusted that the user would see the reference times I label more clearly now. Mostly, I want the readers to understand the seconds-per-division (sec/div) variable. I do want the figure to be legible, but I also want it more to be a quick representational guide to identifying possible abnormal behavior in the flight recordings. If this figure needs to be more legible, please let me know.

11. Fig6. *I thought there were two lines in the graphs of Fig 6.A because the number of troughs overlap. Could you suppress them?*

What was once Figure 6 has been updated to be heatmaps instead of line graphs. These heatmaps are much clearer to read and identify noise with.

12. L498. *Should it be 'continuous flight to bursting' instead of 'bursting to continuous flight'?*

Yes – it has been corrected.

#####

Reviewer #3:

1. *The bibliography is cited in the text using numbers, but in the Reference chapter there are no numbers, so it is very hard to consult the bibliography while reading the document.*

I added reference numbers.

*2. In the introduction it would be interesting to mention alternatives to magnetic levitation, like the use of ball bearings as in [1,2] (see below)*

I really enjoyed reading these pieces you suggested. I added a new introductory paragraph that weighs the pros and cons of different flight mill mechanics.

*References of flight mills using ball bearings:*

=====

*[1] Dubois, G.; Vernon, P.; Brustel, H. A flight mill for large beetles such as *Osmoderma eremita* (Coleoptera: Cetoniidae). In *Saproxyllic Beetles. Their Role And Diversity in European Woodland and Tree Habitats*; PENSOFT Publishers: Sofia, Bulgaria, 2009; pp. 219-224*  
*[2] Martí-Campoy, A.; Ávalos, J.A.; Soto, A.; Rodríguez-Ballester, F.; Martínez-Blay, V.; Malumbres, M.P. Design of a Computerised Flight Mill Device to Measure the Flight Potential of Different Insects. *Sensors* 2016, 16, 485.*

*3. The dimensions of the counterweight are not detailed in the document. Although it is assumed this can be found in Supplemental Figure 1, the author has to clearly state its dimensions or refer to this figure in the text.*

Dimensions of the counterweight will vary based on the weight of the insect. To guide the reader, I added the mass per area ( $\text{g/cm}^2$ ) of the foil in step 1.4.4.

*4. Although the sample frequency of the datalogger can reach up to 40KHz using its four channels (from the technical documentation of the datalogger referred in the paper), the experiment section states the sampling frequency is just 0.1KHz. This is a relatively low frequency and forces the counterweight flag to interrupt the infrared beam for at least 10ms. Did the author calculate the maximum speed an insect can fly without missing turns (turns which are not captured by the datalogger due to a reduced sampling freq)? From the flight angular speed and counterweight flag size a minimum time window can be deduced and some calculations can be carried out to relate max flight speed, flag size and sampling frequency. The author must give some indication on how to tune the width of the counterweight and the minimum sampling frequency for a maximum flying speed. Please, check section 3.2 in [2]. This information is crucial for researchers interested in the use of the described flight mill for a potentially wide range of insects and relates to comments (5) and (6).*

I added a new note describing the minimum width of the counterweight in step 1.4.4. I also tested different low sampling frequencies for this given circular flight path: 0.6283 m. These tests are now plotted in Supplemental Figure 3, and they help researchers decide which sampling frequency best suits their test insect.

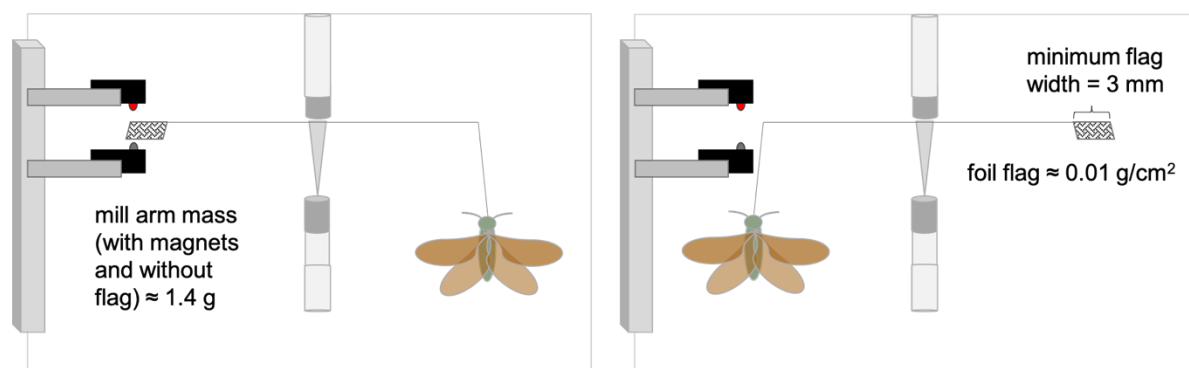
*5. Is the size of the counterweight related to the mass of the insect tethered to the mill? If this is not the case, a combination of a low mass insect and a large counterweight may be too*

*unbalanced to let the insect fly normally, it may affect the rotation of the arm or the effort the insect is required to exert in order to fly. If both are related (as they should be, from this reviewer's point of view) an insect with low mass requires a small counterweight; in this case, will the small counterweight interrupt the infrared beam clearly enough to be recognized?*

Yes, the counterweight is positively related to the mass of the insect tethered to the mill. The diameter of the IR beam is at most 2.4 mm. As long as the flag is at least 2.4 mm wide (3 mm is a much more optimal minimum width), aligned in front of the emitter lens that sends out the beam of IR light as the arm rotates between the sensors, and – this is key – the flag is made out of aluminum (AI flag =  $1\text{e-}4\text{ g/mm}^2$ ), then a clear drop in voltage from around 5V to near 0V will be produced. This drop in voltage will be soundly detectable as a trough in the Python standardize script. However, if the flag is made out of a less reflective material like masking tape, then it will take a much larger flag and multiple layers of material to break the beam. This will then lead to a heavier flight mill arm and a stronger weight imbalance between the flag and the insect on opposite ends of the arm. I added a note in step 1.4.4. that includes these limits.

*6. Related to the size of the insect, could a big enough insect disrupt the beam and count false turns? And also, could a big insect hit the lateral wall? The side of the arm where the insect is attached may be shortened to avoid the insect disrupting the beam or crashing or rubbing some of the elements in the wall, but the other side with the counterweight must keep its length to allow the disruption of the infrared beam. Is there any effect of this asymmetry taken into account in the measurements?*

Adjusting the arm is one way to prevent a big insect from hitting the lateral wall or the sensors. This was a particular issue I bumped into during the first prototype when I noticed that the soapberry bugs were able to reach the sensors with their legs. They then would dismount themselves from the arm. I then found an alternative: making the position of the sensors flexible by 3D printing a linear guide rail and sensor holders. These allow the IR sensors to be realigned at various positions in order to prevent the bug from latching onto a sensor or potentially disrupting the sensor with their own bodies. Another alternative, which is not demonstrated here but could be done in theory, is to redesign a new sensor that could reposition the sensor holder more inwards into the cell. Then, the user can elevate the magnet holders higher and bend the hypodermic tubing even closer to its midpoint so that the insect is far below the sensors. That way, the arms will still be symmetrical. Here is a small schematic diagram to show:



The downside of this alternative is that you may need multiple sensor holder prototypes in order to accommodate different insects. But since the holders can be easily slide in and out of the linear guide rail, it makes it more manageable.

Finally, no effect of asymmetry has been taking into account as of so far. The soapberry bugs were tested on a symmetrical flight mill arm. For bugs of different sizes, this was achieved by 1) moving the sensors up or down so bugs couldn't reach the sensors to dismount themselves and 2) making sure the flag was horizontally balanced with the counterweight flag.

*7. In order to record events from the installation of the eight mills described in the work the use of two dataloggers is needed (from the documentation of the datalogger there is a maximum of four input channels). Is the WinDAQ Software able to seamlessly work with the two dataloggers at the same time? It would be possible to connect more dataloggers to same computer? To have, say, 16 mills?*

Yes, the WinDAQ Software will open a window for each datalogger connected to the computer. Each window can run, collect, and display data simultaneously. Therefore, the only limitation one would have is how many USB ports are free on the computer. If one needed to hook up 16 cells (or two flight mill machines) to a single computer with two data loggers per mill, then the user would either need to invest in a multi-port USB hub or invest in a datalogger that can hold more than four input channels (some have 8 or 16 analog inputs). If the user invests in a 16 analog logger then there is the disadvantage of all cells having to be close to each other because their circuit wires would all connect to one logger. The ideal then would to have two data loggers with 8 inputs, so that each machine can more easily separate from one another if necessary.

*8. The author must indicate the weight of the mobile elements, individually or at least in total. This mass can affect the capacity of the tethered insect to start the flight because of the moment of inertia.*

A flight mill arm (with magnets and without a flag) weighs about 1.4 g. I added this information in step 1.4.4 for the reader. The flag mass can vary based on the mass of the tethered insect.

*References of flight mills using ball bearings:*

=====

- [1] Dubois, G.; Vernon, P.; Brustel, H. A flight mill for large beetles such as *Osmoderma eremita* (Coleoptera: Cetoniidae). In *Saproxyllic Beetles. Their Role And Diversity in European Woodland and Tree Habitats*; PENSOFT Publishers: Sofia, Bulgaria, 2009; pp. 219-224
- [2] Martí-Campoy, A.; Ávalos, J.A.; Soto, A.; Rodríguez-Ballester, F.; Martínez-Blay, V.; Malumbres, M.P. Design of a Computerised Flight Mill Device to Measure the Flight Potential of Different Insects. *Sensors* 2016, 16, 485.

#####

*Reviewer #4:*

*Major Concerns:*

*The manuscript has a clear and focused improvement on a well established technique. Flight mills, despite being around for 6 decades, are still shrouded by rare parts and expertise, not to mention high costs in commercial systems, making them inaccessible to a vast majority of researchers. By using new techniques and open source tools, this protocol democratizes researchers' access to flight mills. Laser cutting coupled with 3d printing enables speed and design complexity simultaneously which individually isn't possible.*

Thank you! The integration of open source tools in science is powerful and exciting.

*1. The manuscript claims the design works with diverse insects sizes which is a great feature. However, this had not been demonstrated. It would be beneficial to provide examples with insects of different sizes/weights, and describe, the adjustments needed in the configuration.*

Valuable suggestion – I added a new figure (Figure 5) that shows how one would go about testing an insect as small as a fruit fly and as large as a soapberry bug or milkweed bug. I show steps where the user would magnetically paint the insects and then show how the insects would look attached to the flight mill arm. In theory, even larger insects would be possible, but this has not been tested, so instead I offer a schematic (see response to Reviewer #3, comment 6).

*2. Secondly, the manuscript does not detail the tethering process itself very easily for replication (section 2.1). The use of the magnetic paint is very clever, but how should you add it? How much of the pronotum should be covered? How do you tether the insects securely and without injury? Does angle of their body or positioning matter? Do you use ice or CO2 as an anesthetic? How do you attach them to the device? This should be explained in more detail for new readers who may have little experience in tethering experiments.*

Figure 5 also shows and describes how to paint different insects without injury. In the figure legend, I give an example of mistakes that can be made if, for instance the insect's field of vision is not taken into account.

*3. Third, the experimentation needs more detail. It is a bit mysterious as of now. For example, in 466-471: "Any individuals that did not exhibit continuous flight behavior at least within the last 10 minutes of its 30 minute testing phase were pulled off the flight mill and replaced with a new bug and its accompanying ID in an event marker comment. All bugs that exhibited continuous flight remained on the flight mill beyond 30 minutes until they stopped flying. Bugs were swapped until 4 PM each day. As represented in Figure 8, flight trials of single individuals in one day's worth of recording varied in length from 30 minutes to 20+ hours and were routinely asynchronous." Please describe the difference between continuous and asynchronous flight in this context to clarify for new users. Is there likely to be a difference between an insect that has flown for 30 minutes vs one for several hours? Does the latter mean you retested insects (since the testing period was 30 minutes), or just kept recording them? Is this variance a good practice for measuring flight behavior?*

Yes, asynchronous flight meant that I gave insects multiple attempts to fly continuously in that 30 min testing phase. However, I realize that the word could be seen as archaic and not as

important as the observation of different flight behaviors, so I removed it. Instead, I defined bursting and continuous flight earlier on in the experimental description (now in the first paragraph of the representative results). This could help clarify why insects were given a 30 min testing phase.

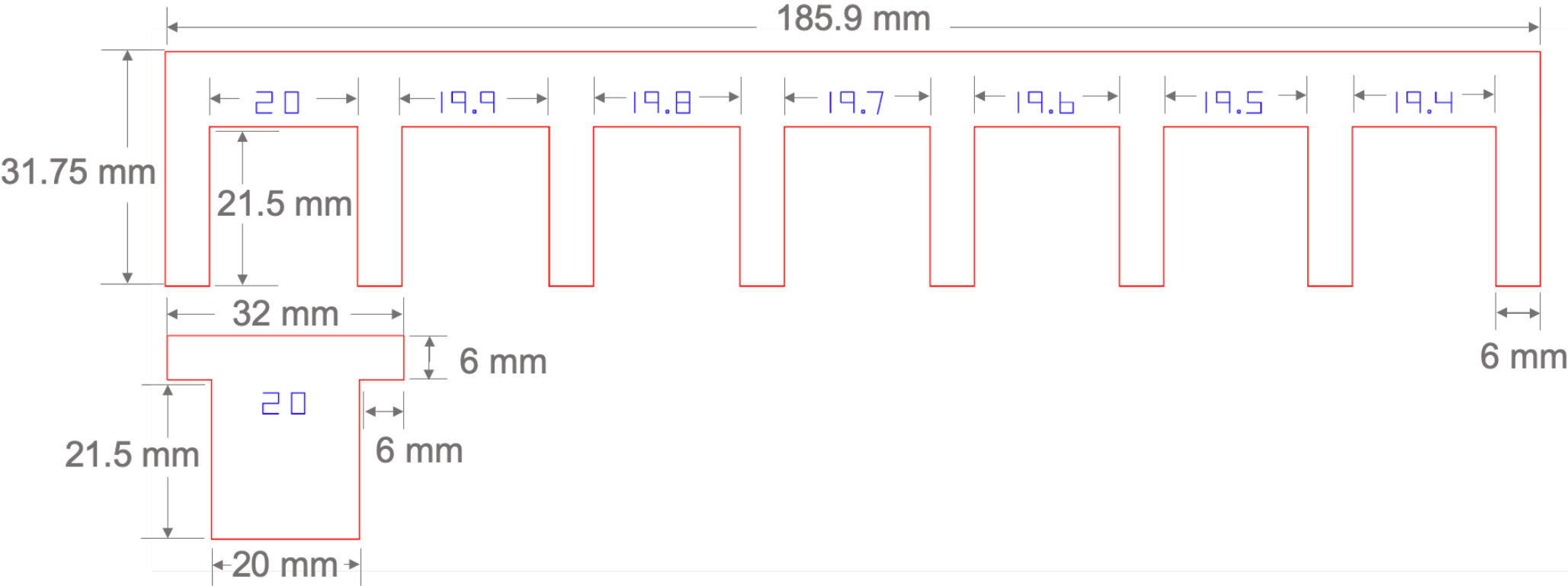
Also, interesting final question – some research will restrict their trial lengths and permit insects to attempt to fly or fly during the whole trial. The approach I took seemed reasonable because soapberry bugs are particularly strong flyers, capable of reaching 14 km of flight distance and 20+ h of continuous flight duration. This sort of stamina is important to capture as well as the frequency of bursting flight within a sample population. However, I do lose some information because of that, such as flight periodicity, because I removed continuous flyers as soon as they stopped flying. So, experimentally it is a trade-off between capturing the full flight capacity of insects and observing flight behavior or strategies. That being said, I now elucidate on this trade-off/alternative experimental setup in the representative results.

*4. Please describe all parts and makes. For example, I couldn't find the details for the IR sensor and data logger components.*

I added new details in steps 1.5.1. and 1.5.2. describing relevant features of the IR sensors and datalogger, respectively.



set\_number



## Input Files

ID	died?	chamber	set_number
9		A-1	6
218		A-2	6
419		A-3	6
262		A-4	6
250		B-1	6
72		B-2	6
2		B-3	6

data/datasheet.csv

TBF voltage reading event\_happened,event\_num date, time event\_marker

"Samples per sec. = 400/1"

```

0.000, 4.90234E+00, 4.93774E+00, 4.89136E+00, 4.94385E+00, 3, 1, 02-24-20, 08:40:36
0.010, 4.90234E+00, 4.93774E+00, 4.89136E+00, 4.94385E+00, 0, 0, 02-24-20, 08:40:36
0.020, 4.90234E+00, 4.93774E+00, 4.89136E+00, 4.94385E+00, 0, 0, 02-24-20, 08:40:36
0.030, 4.90234E+00, 4.93774E+00, 4.89014E+00, 4.94385E+00, 0, 0, 02-24-20, 08:40:36
...
2301.250, 4.84497E+00, 4.93774E+00, 4.88037E+00, 4.94263E+00, 0, 0, 02-24-20, 09:18:57
2301.260, 4.84497E+00, 4.93774E+00, 4.88037E+00, 4.94263E+00, 0, 0, 02-24-20, 09:18:57
2301.270, 4.84497E+00, 4.93774E+00, 4.88037E+00, 4.94263E+00, 0, 0, 02-24-20, 09:18:57
2301.280, 4.84497E+00, 4.93774E+00, 4.88037E+00, 4.94263E+00, 2, 2, 02-24-20, 09:18:57, "158 start"
2301.290, 4.84497E+00, 4.93774E+00, 4.88037E+00, 4.94263E+00, 0, 0, 02-24-20, 09:18:57

```

recordings/\*.TXT

## Process

## functions

## define\_dicts

Creates 2 dictionaries.

## map\_IDs

Uses dictionaries to map IDs from .TXT file event marker comments.

## split\_files

Generates .TXT files that contain the TBF, voltage readings, and datetimes specific to each bug tested.

```

first_flight_dict = { (6, A, 1): 9,
                     (6, A, 2): 218,
                     (6, A, 3): 419,
                     (6, A, 4): 262,
                     (6, B, 1): 250,
                     (6, B, 2): 72,
                     (6, B, 3): 2
                     ...
                     }

current_flight_dict = { (6, A, 9): 1,
                      (6, A, 218): 2,
                      (6, A, 419): 3,
                      (6, A, 262): 4,
                      (6, B, 250): 1,
                      (6, B, 72): 2,
                      (6, B, 2): 3
                      ...
                      }

```

```

.000, 4.90234E+00, 4.93774E+00, 4.89136E+00, 4.94385E+00, 0, 2020-02-24 08:40:36 250,72,2,403
.010, 4.90234E+00, 4.93774E+00, 4.89136E+00, 4.94385E+00, 0, 2020-02-24 08:40:36 250,72,2,403
.020, 4.90234E+00, 4.93774E+00, 4.89136E+00, 4.94385E+00, 0, 2020-02-24 08:40:36 250,72,2,403
.030, 4.90234E+00, 4.93774E+00, 4.89014E+00, 4.94385E+00, 0, 2020-02-24 08:40:36 250,72,2,403
.040, 4.90234E+00, 4.93774E+00, 4.89136E+00, 4.94385E+00, 0, 2020-02-24 08:40:36 250,72,2,403

```

Generates an intermediate file in the files2split folder that maps (by ID) when bugs come in and out of the flight mill for all 4 chambers.

TBF voltage date time

TL\_set006-2-24-2020-B1\_34.txt TL\_set006-2-24-2020-B1\_34.txt

TL\_set006-2-24-2020-B1\_47.txt TL\_set006-2-24-2020-B1\_47.txt

TL\_set006-2-24-2020-B1\_72.txt TL\_set006-2-24-2020-B1\_72.txt

TL\_set006-2-24-2020-B1\_124.txt TL\_set006-2-24-2020-B1\_124.txt

TL\_set006-2-24-2020-B1\_146.txt TL\_set006-2-24-2020-B1\_146.txt

TL\_set006-2-24-2020-B1\_158.txt TL\_set006-2-24-2020-B1\_158.txt

TL\_set006-2-24-2020-B1\_187.txt TL\_set006-2-24-2020-B1\_187.txt

TL\_set006-2-24-2020-B1\_205.txt TL\_set006-2-24-2020-B1\_205.txt

TL\_set006-2-24-2020-B1\_217.txt TL\_set006-2-24-2020-B1\_217.txt

Generates these files by creating a dictionary of lists of dictionaries called ID\_data.

ID is the key to ID\_data

```

ID_data = { 34: [(TBF: 17927.440, voltage: 4.85962E+00, datetime: 2020-02-24 13:39:23),
                 (TBF: 17927.450, voltage: 4.85962E+00, datetime: 2020-02-24 13:39:23),
                 (TBF: 17927.460, voltage: 4.85962E+00, datetime: 2020-02-24 13:39:23),
                 ...]
            ...

```

A list of dictionaries are the values to ID\_data. Each dictionary becomes a row in the final .TXT file.

## standardize\_troughs.py

## Input Files

main\_path = r"Users/&lt;username&gt;/Desktop/Flight\_scripts/"

TBF voltage datetime

```

17927.440, 4.85962E+00, 2020-02-24 13:39:23
17927.450, 4.85962E+00, 2020-02-24 13:39:23
17927.460, 4.85962E+00, 2020-02-24 13:39:23
17927.470, 4.85962E+00, 2020-02-24 13:39:23
17927.480, 4.85962E+00, 2020-02-24 13:39:23

```

split\_files/\*.TXT

## Process

## functions

## trough\_standardize

Identifies large dips in voltage as troughs.

Standardization interval equations and examples:

$$voltage_{min} = voltage_{mean} - dev_{min}$$

$$voltage_{max} = voltage_{mean} + dev_{max}$$

$$x = \frac{voltage(TBF) - voltage_{min}}{voltage_{max} - voltage_{min}}$$

Not a trough:

$$4.78 = 4.79 - 0.01$$

$$4.80 = 4.79 + 0.01$$

$$-2 = \frac{4.74 - 4.78}{4.80 - 4.78}$$

Trough ( $x < -2$ ):

$$-202 = \frac{4.74 - 4.78}{4.80 - 4.78}$$

4.7945

Representative standardization interval - anything that falls outside it is identified as a trough.

## map\_diagnostics

Generates a heat map (.PNG) to diagnose the robustness of the recording file.

A larger standardization interval is more robust and will clearly identify large troughs. A smaller one is more sensitive and may let noise through.



## write\_to\_file

Generates standardized .TXT files that contain the TBF and location of troughs (trough = 1).

```

27273.20, 0.00
27273.21, 0.00
27273.22, 1.00
27273.23, 0.00
27273.24, 0.00

```

Trough at TBF 27273.22 seconds.

## flight\_analysis.py

## Input Files

main\_path = r"Users/&lt;username&gt;/Desktop/Flight\_scripts/"

TBF troughs (0 = no trough; 1 = trough)

```

27273.20, 0.00
27273.21, 0.00
27273.22, 1.00
27273.23, 0.00
27273.24, 0.00

```

standardized\_files/\*.TXT

## Process

## functions

## time\_list

Filters out only for time values where a trough occurs.

[2119.48, 2122.85, 2125.58, 2127.96, 2130.17, 2132.32, 2134.44, ...]

## speed\_list

Corrects for false troughs and calculates the speed between troughs.

Speed calculation depends on the circular flight path.

[0, 1.1186350148368316, 1.3808791208791118, 1.583949798318601, ...]

## distance

Corrects for false troughs and calculates the distance flown and average speed.

ID: 318  
CHAMBER A-2  
Average speed (m/s) -> 1.34  
Total flight time (s) -> 879.86  
Distance (m) -> 610.71  
Shortest flying bout (s) -> 60.28  
Longest flying bout (s) -> 255.23  
This individual spent 0.140 of its time flying with this composition:  
60s-90s = 0.467 with 0 events  
90s-140s = 0.000 with 0 events  
140s-160s = 0.000 with 0 events  
160s-180s = 0.000 with 0 events  
180s-200s = 0.000 with 0 events

## recording\_duration

Calculates the duration of the bug spent flying.

## flying\_bouts

Calculates bout durations and % spent flying.

## graph

Cleans up speed and time columns for easy graphing.

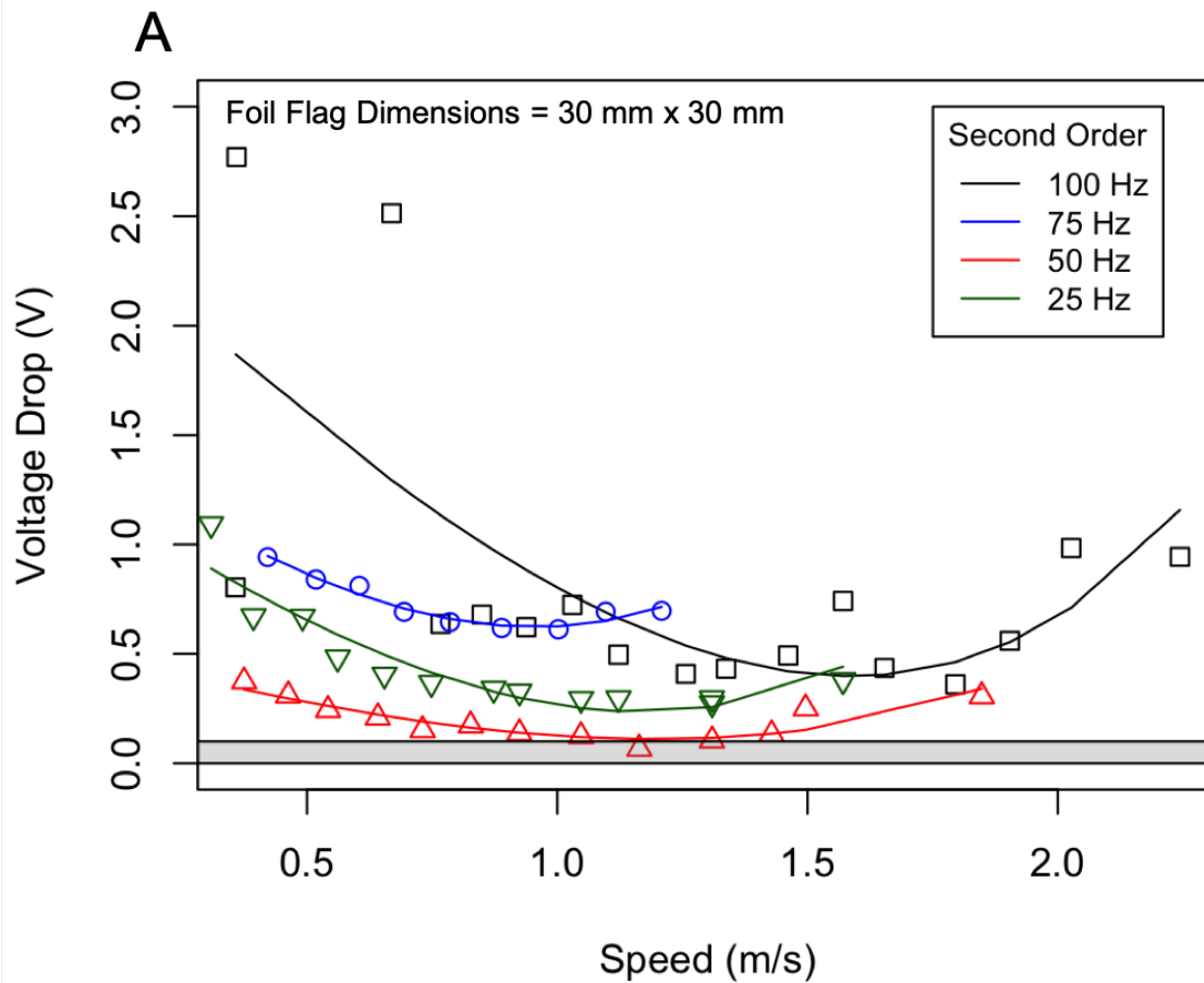
Between bouts, new time and speed data points are added to represent that the insect stopped flying (e.g. 2295.33 s, 0 m/s):

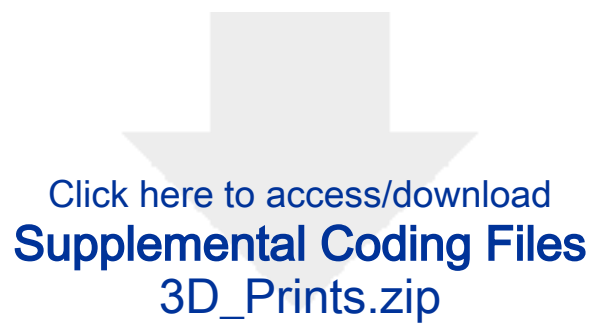
[2122.85, 2125.58, 2126.58, 2294.33, 2295.33, ...]

[1.1186350148368316, 1.3808791208791118, 0, 0, ...]


Generates a flight\_stats\_summary.csv with multiple flight statistics:

ID	filename	trial_type	chamber	channel_letter	channel_num	set_number	average_speed	total_flight_time	distance	shortest_flying_bout	longest_flying_bout	portion_flying	recording_duration	max_speed	
318	set001-2-17-2020-A2_318.txt	T1	A-2	A		2	1	1.34	619.86	610.71	60.28	255.23	0.14	6300.43	1.4
371	set004-2-20-2020-A4_371.txt	T1	A-4	A		4	4	1.24	1834.37	2129.94	91.04	1323.21	0.74	2402.19	1.4
176	set004-2-20-2020-B3_176.txt	T1	B-3	B		3	4	1.17	32.04	22.62	0	29.14	0.01	2347.31	1.3









Click here to access/download  
**Supplemental Coding Files**  
standardize\_troughs.py



Click here to access/download  
**Supplemental Coding Files**  
flight\_analysis.py